

Provided for non-commercial research and educational use only.  
Not for reproduction or distribution or commercial use.



This article was originally published in a journal published by Elsevier, and the attached copy is provided by Elsevier for the author's benefit and for the benefit of the author's institution, for non-commercial research and educational use including without limitation use in instruction at your institution, sending it to specific colleagues that you know, and providing a copy to your institution's administrator.

All other uses, reproduction and distribution, including without limitation commercial reprints, selling or licensing copies or access, or posting on open internet sites, your personal or institution's website or repository, are prohibited. For exceptions, permission may be sought for such use through Elsevier's permissions site at:

<http://www.elsevier.com/locate/permissionusematerial>



# The use of slow manifolds in reactive flows

Zhuyin Ren <sup>\*</sup>, Stephen B. Pope

*Sibley School of Mechanical & Aerospace Engineering, Cornell University, Ithaca, NY 14853, USA*

Received 19 May 2006; received in revised form 6 September 2006; accepted 19 September 2006

Available online 27 October 2006

---

## Abstract

In calculations of chemically reactive flows, dimension reduction of reactive systems via the use of slow attracting manifolds is an effective approach to reducing the computational burden. In the reduced description, the reactive system is described in terms of a smaller number of reduced composition variables (e.g., some major species) instead of the full composition (i.e., the full set of chemical species), and the evolution equations for the reduced composition variables are solved. In this work, we address the issues arising from the use of chemistry-based slow manifolds in inhomogeneous reactive flows. Chemistry-based slow manifolds are identified (or constructed) based solely on chemical kinetics (i.e., based on homogeneous reactive systems) without accounting for transport processes such as convection and molecular diffusion. For a class of reaction–diffusion systems, by perturbation analysis, it is shown that three different mechanisms contribute to pulling compositions off the chemistry-based slow manifolds, namely, noninvariance, dissipation–curvature, and differential diffusion effects. As the names indicate, these mechanisms contribute, respectively, if the manifold is not invariant; if the manifold is curved (and there is nonzero molecular diffusion); and if the diffusivities of the species differ. In the regime where the fast chemical time scales are smaller than the physical time scales, the composition perturbations off the slow manifold by these three mechanisms are small. However, these three seemingly small perturbations introduce three generally nontrivial terms into the governing equations for the reduced compositions, which in general are of leading order. Moreover, for the convection–reaction–diffusion systems, we validate the close-parallel assumption [Z. Ren, S.B. Pope, A. Vladimirov, J.M. Guckenheimer, *Proc. Combust. Inst.* (2007), doi:10.1016/j.proci.2006.07.106] to account for these effects in the reduced description. It is shown that with the use of the close-parallel assumption, the reduced description agrees well with the full reactive system. Different scenarios where these three effects could be neglected are also discussed.

© 2006 The Combustion Institute. Published by Elsevier Inc. All rights reserved.

*Keywords:* Slow manifold; Transport–chemistry coupling; Dimension reduction; Close-parallel; Chemical kinetics

---

## 1. Introduction

A wide variety of chemically reactive flows involve a large number of chemical species, which par-

ticipate in tens to thousands of elementary chemical reactions occurring simultaneously within a complex flow field. These processes are modeled by a large set of partial differential equations (PDEs) representing the evolution of chemical species and energy, coupled with the Navier–Stokes equations. One challenging feature of chemical kinetics is the presence of a wide range of time scales, which adds a dramatic compu-

---

<sup>\*</sup> Corresponding author. Fax: +1 (607) 255 1222.  
E-mail address: [zr26@cornell.edu](mailto:zr26@cornell.edu) (Z. Ren).

tational burden and makes the direct use of detailed chemical kinetics computationally expensive. Hence, there is a well-recognized need to develop methods that rationally reduce the computational burden imposed by the direct use of detailed chemical kinetics in the calculations of reactive flows.

For a transient homogeneous reactive flow (in the absence of transport processes such as convection and molecular diffusion) that is described by a set of ordinary differential equations (ODEs), the time-dependent solution corresponds to a reaction trajectory in the composition space. Due to the fast time scales in chemical kinetics, all the reaction trajectories quickly relax to a low-dimensional slow manifold in the composition space [1–9]. Based on this observation, dimension reduction and hence the reduced description of the reactive flows via the use of low-dimensional manifolds are widely used to effectively reduce the computational burden [1–23]. For example, techniques such as intrinsic low-dimensional manifolds (ILDM) [1], the quasi-steady-state assumption (QSSA) [10–13], computational singular perturbation (CSP) [21–23], the zero derivative principle method [16,17], and the ICE-PIC method [9] explicitly or implicitly identify a low-dimensional manifold in the composition space (as an approximation to a slow attracting manifold) to represent the reactive system. In the reduced description, the reactive system is described in terms of a smaller number of reduced composition variables (e.g., some major species), and the evolution equations for the reduced composition variables are solved.

The dimension reduction for homogeneous reactive flows has achieved great success in the past 20 years. However, most realistic reactive flows are inhomogeneous and involve transport processes such as convection and molecular diffusion. The reduced description of inhomogeneous flows via the use of slow manifolds is greatly complicated by the transport processes present and the coupling between chemistry and the transport processes. Substantial studies on how and when the transport processes can affect the compositions and the reduced description of the reactive flows have been performed in Refs. [18,22–44]. Currently, there are two distinct approaches to provide a reduced description of the inhomogeneous reactive flows.

In the first approach the slow manifold (which is explicitly or implicitly identified) is based on the governing PDEs, which include convection, diffusion, and reaction [22,23,25,27–39]. The transport–chemistry coupling is incorporated into the construction of the slow manifolds. For example, in Ref. [35], Bongers et al. identify a manifold in an augmented space consisting of both the compositions and composition fluxes. In Refs. [38,39], Davis considers low-

dimensional manifolds in the infinite-dimensional function space for reaction–diffusion systems. In Ref. [34], after the initial transient, by equilibrating the transport process and reactions in the fast subspace, Singh et al. obtain a set of differential algebraic equations (involving transport processes such as molecular diffusion), which defines an infinite-dimensional slow manifold in function space. Similarly, in Refs. [22,23,25,27–29], when CSP is extended to inhomogeneous flows, a similar set of differential equations defining a slow manifold can be obtained. One thing worthy of mention is that the slow manifolds defined by these differential (or differential algebraic) equations are difficult to compute due both to the spatial information needed and to the change of slow and fast directions in the composition space (with possible discontinuities).

In the second approach the slow manifold is a low-dimensional manifold in the finite-dimensional composition space and is identified solely based on chemical kinetics without accounting for transport processes [12,24,41,42]: we refer to such manifolds as “chemistry-based.” Hence all the existing methods and algorithms for homogeneous systems can be straightforwardly applied. In the reduced description, the transport–chemistry coupling either is accounted for by projecting transport processes back onto the low-dimensional manifold or is simply neglected, as is done in the QSSA method [12,45,46]. The use of chemistry-based slow manifolds to describe inhomogeneous flows is expected to be adequate in the regime where the fast chemical time scales are smaller than the transport time scales [29]. This is the case for typical combustion processes. Two examples in this approach are the extension of the ILDM method [41,42] and the ICE-PIC method to inhomogeneous reactive flows [24].

Consequently, the formulation of reduced descriptions of reactive flows from the above two approaches is different. For example, in the CSP or ASIM method, the reduced description may be given by a set of PDEs for the reduced composition variables supplemented by differential (or differential algebraic) equations defining a manifold. On the boundaries, the full composition is provided. During the calculation, all the equations have to be solved together and this is in general computationally expensive. In contrast, in the ILDM and ICE-PIC methods, the reduced description is given by a set of PDEs for the reduced composition variables, in which the terms arising can be evaluated on the chemistry-based manifold. On the boundaries, only the reduced composition needs to be provided. Given the reduced composition, the manifold point can either be retrieved from a precomputed table containing the manifold information, or be obtained through a local computation. In the local

computation of the manifold, no spatial information is needed.

This paper focuses on the use of chemistry-based slow manifolds to describe inhomogeneous reactive flows. As mentioned earlier, the slow manifold employed is identified solely based on chemical kinetics, i.e., based on homogeneous systems governed by a set of ODEs. Chemistry-based manifolds can be categorized based on whether or not they are invariant. By definition, a chemistry-based manifold is invariant if the reaction trajectory from any point in the manifold remains in the manifold. In homogeneous reactive flows, for invariant manifolds, with the full composition being on the manifold, the rate of change of the reduced composition variables is determined by the full chemical kinetics without approximation; whereas, for noninvariant manifolds, the rate of change of the reduced composition variables depends strongly on the choice of the projection used to project the full rate-of-change vector onto the manifold (see Refs. [1,47]). Thus, being invariant is a highly desirable property. (Moreover, it is also desirable for the manifold to be attractive; see Refs. [48,49].) Among existing dimension-reduction methods, trajectory-generated low-dimensional manifolds (TGLDM) [2,3], the Roussel and Fraser algorithm (RF) [4–6,18], the method of invariant manifolds [19,20], the ICE-PIC method [9], and other iterative techniques as discussed in Refs. [20,30] fall into the class of methods that identify chemistry-based invariant manifolds.

Besides the noninvariance difficulty (if the slow manifold is not invariant), the use of chemistry-based slow manifolds in inhomogeneous flows is complicated by the transport processes present and the coupling between chemistry and these transport processes. Even through an inhomogeneous reactive flow with arbitrary initial conditions can admit an infinite number of time scales associated with the transport processes such as molecular diffusion, for a particular flow a finite number of transport time scales can be identified based on the given composition distribution [50,51]. For typical [1] combustion processes, chemical kinetics have a much wider range of time scales than those of transport processes. It is believed that due to the fast chemical time scales, all the compositions in inhomogeneous reactive flows (after an initial transient and far from the boundaries) still lie close to a low-dimensional chemistry-based attracting manifold. Previous studies [18,26,29,33,41,42,44] confirm that the compositions in inhomogeneous reactive flows are not exactly on, but are close to chemistry-based slow manifolds. Transport processes such as molecular diffusion may tend to draw the composition off the slow manifold, whereas the fast processes in chemistry relax the perturba-

tions back toward the slow manifold. Previous studies have also pointed out some mechanisms that pull compositions off the chemistry-based slow manifold, such as the dissipation–curvature mechanism found in Ref. [44]. However, a systematic study of the mechanisms that may draw compositions off the chemistry-based slow manifold is still not available. Also, questions remain on how to quantify the transport effects on the compositions. As far as the evolution of the reduced composition is concerned, a set of PDEs for the reduced compositions can be deduced from those for the full composition. However, in order for this set of equations to be closed, it is necessary to introduce assumptions or approximations. Based on time-scale analysis, previous studies [22,41] suggest that the transport–chemistry coupling could be accounted for and thus the accurate evolution equation can be obtained by projecting the transport and reaction processes onto the slow subspaces identified in each individual approach. However, no attempts have been made in Refs. [22,41] to understand and quantify the relation between the departure of compositions from the chemistry-based slow manifold and the consequent transport–chemistry coupling. In this study, we deduce the evolution equations for the reduced compositions by exploring the relation between the departure of compositions and the consequent transport–chemistry coupling. The major contributions of the paper are the identification of all the possible mechanisms through which transport processes act on both composition and the reduced description; clarification and quantification of the composition departure and the resulting transport–chemistry coupling; and verification of the close-parallel assumption by Ren et al. [24] to quantify the transport effect and to account for the transport–chemistry coupling in the reduced description.

In this paper, we introduce a model reaction–diffusion system, for which an asymptotic analysis is performed. This confirms the conclusions reached in [22,24,25,29,41,42] that, in general, a common practice referred to as the “first approximation” is not valid. This first-approximation approach amounts to the complete neglect of departures from the manifold, and therefore the complete neglect of the transport–chemistry coupling in the reduced description. Instead, the exact PDEs for the reduced compositions contain three additional terms that in general are of leading order. These three terms are referred to as noninvariance, dissipation–curvature, and differential diffusion. As the names indicate, these terms represent effects that arise, respectively, if the manifold is not invariant; if the manifold is curved (and there is nonzero molecular diffusion); and if the diffusivities of the species differ.



In previous work [24] we obtained a closed set of PDEs for the reduced compositions by invoking the close-parallel assumption, namely that compositions that occur in a reacting flow lie close to and evolve parallel to the low-dimensional chemistry-based manifold used in the reduced description. In this paper, we show that the close-parallel assumption leads to the correct PDE for the model systems.

The outline of the remainder of the paper is as follows. In Section 2, we provide a brief overview of the reduced description of reactive flows via slow manifolds. In Section 3, we consider a class of reaction–diffusion models and derive the accurate evolution equation for the reduced composition variable by perturbation analysis. The noninvariance, dissipation–curvature, and differential diffusion effects are revealed. In Section 4, we validate the close-parallel assumption to account for these effects in the reduced description. Conclusions are drawn in Section 5.

## 2. Reduced description of inhomogeneous reactive flows

To demonstrate the reduced description, we consider an inhomogeneous reactive flow, where the pressure  $p$  and enthalpy  $h$  are taken to be constant and uniform (although the extension to variable pressure and enthalpy is straightforward). The system at time  $t$  is then fully described by the full composition  $\mathbf{z}(\mathbf{x}, t)$ , which varies both in space,  $\mathbf{x}$ , and in time,  $t$ . The full composition  $\mathbf{z}$  can be taken to be the mass fractions of the  $n_s$  species or the specific species moles (mass fractions divided by the corresponding species molecular weights). The system evolves according to the set of  $n_s$  PDEs

$$\frac{\partial}{\partial t} \mathbf{z}(\mathbf{x}, t) + v_i \frac{\partial \mathbf{z}}{\partial x_i} = \mathbf{D} \{ \mathbf{z}(\mathbf{x}, t) \} + \mathbf{S}(\mathbf{z}(\mathbf{x}, t)), \quad (1)$$

where  $\mathbf{S}$  denotes the rate of change of the full composition due to chemical reactions. The spatial transport includes the convective contribution ( $v_i \frac{\partial \mathbf{z}}{\partial x_i}$ , where  $\mathbf{v}(\mathbf{x}, t)$  is the velocity field) and the diffusive contribution ( $\mathbf{D}$ ). In calculations of reactive flows, one simplified model widely used for diffusion is

$$\mathbf{D} \{ \mathbf{z} \} = \frac{1}{\rho} \nabla \cdot (\rho \mathbf{\Gamma} \nabla \mathbf{z}), \quad (2)$$

where  $\rho$  is mixture density and  $\mathbf{\Gamma}$  is a diagonal matrix with the diagonal components  $\Gamma_1, \Gamma_2, \dots, \Gamma_{n_s}$  being the mixture-averaged species diffusivities, which are usually functions of  $\mathbf{z}$ .

In the reduced description, the reactive system is described in terms of a smaller number  $n_r$  of reduced composition variables  $\mathbf{r}(\mathbf{x}, t) = \{r_1, r_2, \dots, r_{n_r}\}$ , which can be taken to be the mass fractions (or the

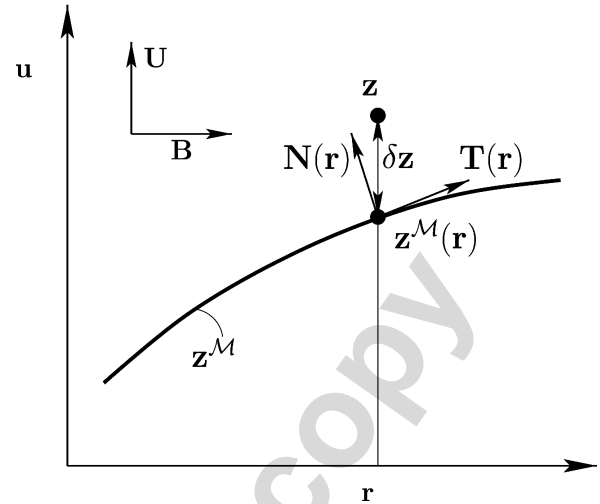


Fig. 1. A sketch in the composition space showing the representation of the general composition as  $\mathbf{z} = \mathbf{z}^{\mathcal{M}} + \delta \mathbf{z}$ . The axes denote the reduced composition  $\mathbf{r}$  (in the subspace  $\text{span}(\mathbf{B})$ ) and the unrepresented variables  $\mathbf{u}$  (in the subspace  $\text{span}(\mathbf{U}) = \text{span}(\mathbf{B})^{\perp}$ ). Also shown are the tangent subspace  $\text{span}(\mathbf{T}(\mathbf{r}))$  and the normal subspace  $\text{span}(\mathbf{N}(\mathbf{r}))$ .

specific moles) of some species and linear combinations of the species (depending on the different methods). In general, the reduced composition  $\mathbf{r}(\mathbf{x}, t)$  can be expressed as

$$\mathbf{r}(\mathbf{x}, t) = \mathbf{B}^T \mathbf{z}(\mathbf{x}, t), \quad (3)$$

where  $\mathbf{B}$  is an  $n_s \times n_r$  constant matrix. For example, if  $\mathbf{r}$  consists of specified “major” species, then each column of  $\mathbf{B}$  is a unit vector consisting of a single entry (unity) in the row corresponding to a major species. But more generally, Eq. (3) allows for linear combination of species. It is in fact the subspace spanned by  $\mathbf{B}$  that is significant, not the particular form of  $\mathbf{B}$ . Hence, without loss of generality, and for simplicity of the following exposition, we take  $\mathbf{B}$  to be orthonormal. Thus, as illustrated in Fig. 1, the full  $n_s$ -dimensional composition space can be decomposed into an  $n_r$ -dimensional represented subspace (spanned by the columns of  $\mathbf{B}$ ) and an  $n_u$ -dimensional unrepresented subspace (spanned by the columns of  $\mathbf{U}$ , with  $\mathbf{U}$  being a constant  $n_s \times n_u$  orthonormal matrix spanning  $\text{span}(\mathbf{B})^{\perp}$  with  $n_u = n_s - n_r$ ). The matrices  $\mathbf{B}$  and  $\mathbf{U}$  satisfy  $\mathbf{B}^T \mathbf{U} = 0$  and  $\mathbf{B} \mathbf{B}^T + \mathbf{U} \mathbf{U}^T = \mathbf{I}_{n_s \times n_s}$ . We define the unrepresented variables to be

$$\mathbf{u}(\mathbf{x}, t) = \mathbf{U}^T \mathbf{z}(\mathbf{x}, t). \quad (4)$$

The  $n_r$ -dimensional chemistry-based manifold  $\mathcal{M}$  used in the dimension reduction is assumed to be the graph of a function of  $\mathbf{r}$ , i.e.,

$$\mathcal{M} = \{ \mathbf{z} \mid \mathbf{z} = \mathbf{z}^{\mathcal{M}}(\mathbf{r}) = \mathbf{B} \mathbf{r} + \mathbf{U} \mathbf{u}^{\mathcal{M}}(\mathbf{r}) \}, \quad (5)$$

for some function  $\mathbf{u}^{\mathcal{M}}(\mathbf{r})$ . One important aspect of the reduced description (not discussed in the paper) is

the choice of the reduced representation, i.e., the specification of  $n_r$  and  $\mathbf{B}$ . For the purpose of this study, both  $n_r$  and  $\mathbf{B}$  are user-specified. Some studies on this topic can be found in Refs. [8,22,52].

In an inhomogeneous reactive system, the full compositions can be expressed as

$$\mathbf{z}(\mathbf{x}, t) = \mathbf{z}^{\mathcal{M}}(\mathbf{r}(\mathbf{x}, t)) + \delta\mathbf{z}(\mathbf{x}, t), \quad (6)$$

where  $\delta\mathbf{z}(\mathbf{x}, t)$  is the departure from the low-dimensional manifold (which may be introduced by initial and boundary conditions, molecular diffusion, and noninvariance). With this representation, as illustrated in Fig. 1, the departure is defined to be in the unrepresented subspace, i.e.,

$$\delta\mathbf{z} = \mathbf{U}\delta\mathbf{u}, \quad (7)$$

where

$$\delta\mathbf{u} = \mathbf{U}^T[\mathbf{z}(\mathbf{x}, t) - \mathbf{z}^{\mathcal{M}}(\mathbf{r}(\mathbf{x}, t))]. \quad (8)$$

Without loss of information, the governing equation, Eq. (1), can be premultiplied by the matrix  $[\mathbf{B} \ \mathbf{U}]^T$  to yield

$$\begin{aligned} \frac{\partial}{\partial t} \begin{bmatrix} \mathbf{r} \\ \mathbf{u} \end{bmatrix} + v_i \frac{\partial}{\partial x_i} \begin{bmatrix} \mathbf{r} \\ \mathbf{u} \end{bmatrix} \\ = \begin{bmatrix} \mathbf{B}^T \mathbf{D} \\ \mathbf{U}^T \mathbf{D} \end{bmatrix} + \begin{bmatrix} \mathbf{B}^T \mathbf{S}(\mathbf{z}) \\ \mathbf{U}^T \mathbf{S}(\mathbf{z}) \end{bmatrix}. \end{aligned} \quad (9)$$

Hence when the reduced composition variables are used to represent the reacting system, the exact evolution equation for  $\mathbf{r}(\mathbf{x}, t)$  is

$$\frac{\partial \mathbf{r}}{\partial t} + v_i \frac{\partial \mathbf{r}}{\partial x_i} = \mathbf{B}^T \mathbf{D}\{\mathbf{z}\} + \mathbf{B}^T \mathbf{S}(\mathbf{z}). \quad (10)$$

In the reduced description, the task is to express the right-hand side of Eq. (10),  $(\mathbf{B}^T \mathbf{D}\{\mathbf{z}\} + \mathbf{B}^T \mathbf{S}(\mathbf{z}))$ , as a function of  $\mathbf{r}$ . The most straightforward approach, denoted as the “first approximation” in Ref. [24], is to completely neglect the departures  $\delta\mathbf{z}$  and assume that the compositions in the reactive flow lie on this chemistry-based manifold, i.e.,

$$\mathbf{z}(\mathbf{x}, t) = \mathbf{z}^{\mathcal{M}}(\mathbf{r}(\mathbf{x}, t)). \quad (11)$$

Hence the evolution equation for the reduced composition variables according to the “first approximation” is

$$\frac{\partial \mathbf{r}}{\partial t} + v_i \frac{\partial \mathbf{r}}{\partial x_i} = \mathbf{B}^T \mathbf{D}\{\mathbf{z}^{\mathcal{M}}(\mathbf{r})\} + \mathbf{B}^T \mathbf{S}(\mathbf{z}^{\mathcal{M}}(\mathbf{r})). \quad (12)$$

As shown below, for a model problem, the “first approximation” is not valid in general, even when Eq. (11) is a valid approximation. It is valid only under some particular circumstances.

In general reactive flows, the accessed compositions are not exactly on the chemistry-based slow manifold. The following factors may cause the compositions to depart from the manifold:

- The chemistry-based slow manifold being not invariant. For some widely used dimension-reduction method such as QSSA and ILDM, the low-dimensional manifolds employed are not invariant.
- The transport processes such as molecular diffusion (see Ref. [44]).
- Initial compositions not lying on the chemistry-based slow manifold. After the initial transient, due to the fast chemical time scales, the compositions are expected to approach the slow manifold.
- The boundary conditions not lying on the chemistry-based slow manifold. Thin boundary layers are expected to be formed adjacent to the boundaries [26,27]. In the boundary layers, the compositions may not be on the slow manifold no matter how faster the fast chemical time scales are. However, far from the boundaries, the compositions are expected to lie close to the slow manifold. These phenomena have been observed by Goussis et al. [29].

The effect of initial and boundary conditions on the reduced description via the use of slow manifold has been studied in Refs. [26,27]. In this study, we focus on investigating the noninvariance effect and the transport effects on the compositions and on the reduced description. As pointed out in Refs. [42,44], the convection process in PDEs does not pull compositions off any chemistry-based manifold. In fact, from the Lagrangian point of view, it is obvious that the convection process alone does not even change the composition of a fluid particle. Hence in this study, we mainly focus on reaction–diffusion systems instead of convection–reaction–diffusion systems. A discussion on the effect of convection on the reduced description is given in Section 4.4. To fulfill the purpose of this study, for all the systems considered, both the initial and boundary compositions are specified to be exactly on the chemistry-based slow manifold considered. (Notice that when the ICE-PIC method [24] is used in the reduced description of reactive flows, the represented variables can be chosen such that the boundary and initial compositions are on the chemistry-based slow manifold.)

### 3. Noninvariance effect and transport–chemistry coupling in reaction–diffusion systems

In this section, for a class of reaction–diffusion systems, by perturbation analysis, we derive the exact evolution equation for the reduced composition variables. The nontrivial terms in the reduced description introduced by noninvariance of the slow manifold and molecular diffusion are identified.

The unsteady reaction–diffusion system in  $\mathbf{x}$ – $t$  space considered evolves according to the PDEs

$$\begin{aligned}\frac{\partial z_1}{\partial t} &= c \frac{z_2 - f(z_1)}{\varepsilon} + g_1(z_1, z_2) + \nabla \cdot (D_1 \nabla z_1), \\ \frac{\partial z_2}{\partial t} &= -\frac{z_2 - f(z_1)}{\varepsilon} + g_2(z_1, z_2) + \nabla \cdot (D_2 \nabla z_2),\end{aligned}\quad (13)$$

where  $\mathbf{z} = \begin{bmatrix} z_1 \\ z_2 \end{bmatrix}$  is the full composition,  $t$  is a normalized (i.e., nondimensional) time,  $\varepsilon \ll 1$  is a small parameter,  $c$  is a positive constant (may be 0,  $\mathcal{O}(\varepsilon)$  or  $\mathcal{O}(1)$ ) that describes the coupling between  $z_1$  and the fast chemistry, and  $D_1$  and  $D_2$  (in general dependent on  $\mathbf{z}$ ) are the diffusivities of  $z_1$  and  $z_2$ , respectively. In Eq. (13),  $f(z_1)$ ,  $g_1(z_1, z_2)$ , and  $g_2(z_1, z_2)$  are assumed to be on the order of 1. The chemical reactions have a large linear contribution from the fast chemistry (represented by the terms  $c \frac{z_2 - f(z_1)}{\varepsilon}$  and  $-\frac{z_2 - f(z_1)}{\varepsilon}$ ) and another generally nonlinear contribution from the slow chemistry (represented by  $g_1(z_1, z_2)$  and  $g_2(z_1, z_2)$ ). The Jacobian matrix from reaction source terms is

$$\mathbf{J} = \frac{1}{\varepsilon} \begin{bmatrix} -cf' & c \\ f' & -1 \end{bmatrix} + \mathcal{O}(1), \quad (14)$$

where  $f'(z_1) \equiv df(z_1)/dz_1$ . The eigenvalue associated with the fast chemical time scale is  $-(1 + cf')/\varepsilon + \mathcal{O}(1)$ , where the function  $f(z_1)$  is specified so that  $(1 + cf')$  is positive (and of order unity) and hence there are slow attracting manifolds in the system. The fast chemical time scale in the system is  $\mathcal{O}(\varepsilon)$ . This set of PDEs is also studied by Lam in the computational singular perturbation (CSP) context [26].

For this system, depending on the methods used, different chemistry-based slow attracting manifolds can be identified. Among them, a valid slow attracting manifold that can be easily identified and employed in the reduced description is

$$\mathbf{z} = \begin{bmatrix} z_1 \\ z_2 \end{bmatrix} = \mathbf{z}^{\mathcal{M}}(z_1) = \begin{bmatrix} z_1 \\ f(z_1) \end{bmatrix}. \quad (15)$$

The tangent unit vector of the slow manifold is  $\mathbf{T} = \frac{1}{\sqrt{1+f'^2}} \begin{bmatrix} 1 \\ f'(z_1) \end{bmatrix}$  and the normal unit vector is  $\mathbf{N} = \frac{1}{\sqrt{1+f'^2}} \begin{bmatrix} -f'(z_1) \\ 1 \end{bmatrix}$ . Moreover, this chemistry-based slow manifold is invariant if the condition

$$\begin{bmatrix} g_1(z_1, z_2) \\ g_2(z_1, z_2) \end{bmatrix} = k(z_1, z_2) \begin{bmatrix} 1 \\ f'(z_1) \end{bmatrix} \quad (16)$$

is satisfied on the manifold, where  $k(z_1, z_2)$  is any function of  $z_1$  and  $z_2$ . The condition basically is a statement of the invariance requirement that the vector  $[g_1 \ g_2]^T$  be in the tangent space of the chemistry-based manifold. Clearly, this condition is not gener-

ally satisfied (i.e., it is not satisfied for a general specification of  $g_1$  and  $g_2$ ).

The unsteady reaction–diffusion system (Eq. (13)) is well posed given the boundary conditions and initial conditions. In this study, both the initial and boundary compositions for the governing PDEs (Eq. (13)) are taken to be exactly on the slow manifold (Eq. (15)).

In the reduced description,  $z_1$  is chosen as the reduced composition variable to represent the reaction–diffusion system. Hence the represented subspace is spanned by  $\mathbf{B} = \begin{bmatrix} 1 \\ 0 \end{bmatrix}$  and the unrepresented subspace is spanned by  $\mathbf{U} = \begin{bmatrix} 0 \\ 1 \end{bmatrix}$ .

### 3.1. Composition perturbation in inhomogeneous reactive flows

By multiplying with  $\varepsilon$ , Eq. (13) can be written as

$$\begin{aligned}\varepsilon \frac{\partial z_1}{\partial t} &= c(z_2 - f(z_1)) + \varepsilon g_1(z_1, z_2) \\ &\quad + \varepsilon \nabla \cdot (D_1 \nabla z_1), \\ \varepsilon \frac{\partial z_2}{\partial t} &= -(z_2 - f(z_1)) + \varepsilon g_2(z_1, z_2) \\ &\quad + \varepsilon \nabla \cdot (D_2 \nabla z_2).\end{aligned}\quad (17)$$

With  $L_1$  and  $L_2$  being the characteristic diffusion length scales of  $z_1$  and  $z_2$ , respectively, we assume the fast chemical time scales are much smaller than the diffusion time scales, i.e.,  $L_1^2/(D_1\varepsilon) \gg 1$  and  $L_2^2/(D_2\varepsilon) \gg 1$ . We further assume  $z_2$  to be a function of  $\mathbf{x}$ ,  $t$ , and  $\varepsilon$ , and that it can be expressed as the perturbation series

$$z_2(\mathbf{x}, t, \varepsilon) = f_0(\mathbf{x}, t) + \varepsilon f_1(\mathbf{x}, t) + o(\varepsilon), \quad (18)$$

with  $\lim_{\varepsilon \rightarrow 0} o(\varepsilon)/\varepsilon = 0$ . To obtain the first term in this series, we set  $\varepsilon = 0$  in Eq. (17) to obtain

$$\begin{aligned}0 &= c(z_2 - f(z_1)), \\ 0 &= -(z_2 - f(z_1)).\end{aligned}\quad (19)$$

Hence  $z_2(\mathbf{x}, t, 0) = f(z_1)$ , i.e.,

$$f_0(\mathbf{x}, t) = f(z_1). \quad (20)$$

This leading order solution is consistent only if the initial conditions and boundary conditions are on the manifold as we assume. (If the initial conditions and boundary conditions are not on the manifold, this leading order solution is valid away from the thin boundary layers close to the boundaries after the initial transient.)

Substituting  $z_2(\mathbf{x}, t, \varepsilon) = f(z_1) + \varepsilon f_1(\mathbf{x}, t) + o(\varepsilon)$  into Eq. (17), and neglecting terms of order  $\varepsilon^2$  and

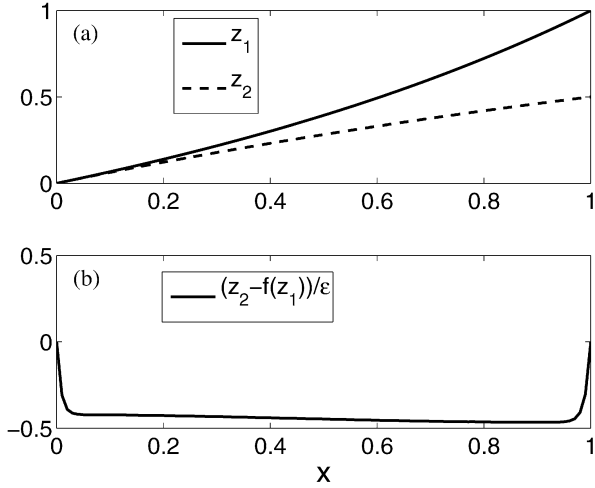


Fig. 2. Results for Case 2 in Table 1 with  $\epsilon = 1 \times 10^{-4}$  and  $D_1 = 1$ . (a) Steady state distribution of  $z_1$  and  $z_2$  against  $x$ ; (b) the normalized perturbation off the slow manifold ( $f(z_1) = z_1/(1 + az_1)$ ). The figure illustrates the boundary layers of the composition perturbation.

higher, we obtain

$$\begin{aligned} \frac{\partial z_1}{\partial t} &= cf_1 + g_1(z_1, f(z_1)) + \nabla \cdot (D_1 \nabla z_1), \\ \frac{\partial f(z_1)}{\partial t} &= -f_1 + g_2(z_1, f(z_1)) \\ &\quad + \nabla \cdot (D_2 \nabla (f(z_1) + \epsilon f_1)). \end{aligned} \quad (21)$$

Now the term  $\partial f(z_1)/\partial t$  can be reexpressed as  $f'(z_1)\partial z_1/\partial t$ . Thus, by multiplying the first equation by  $f'$  and subtracting for the second,  $\partial z_1/\partial t$  is eliminated to yield an expression for  $f_1(\mathbf{x}, t)$ :

$$\begin{aligned} \epsilon \nabla \cdot (D_2 \nabla f_1) &= (1 + cf')f_1 - g_2(z_1, f(z_1)) + f'g_1(z_1, f(z_1)) \\ &\quad - \nabla \cdot (D_2 \nabla f(z_1)) + f' \nabla \cdot (D_1 \nabla z_1). \end{aligned} \quad (22)$$

The order of the term  $\epsilon \nabla \cdot (D_2 \nabla f_1(\mathbf{x}, t))$  needs more consideration. At the boundaries,  $f_1(\mathbf{x}, t) = 0$  given that the boundary compositions are on the slow manifold; away from the boundaries,  $f_1(\mathbf{x}, t)$  is  $\mathcal{O}(1)$ . As a result (see Fig. 2), close to the boundaries,  $f_1$  forms boundary layers of thickness  $\sqrt{D_2 \epsilon}$ . Inside the boundary layers,  $\epsilon \nabla \cdot (D_2 \nabla f_1(\mathbf{x}, t))$  is on the order of 1; away from the boundaries, this term is order of  $\epsilon$  and negligible. Hence for regions away from the boundaries, an explicit expression for  $f_1(\mathbf{x}, t)$  can be obtained,

$$\begin{aligned} f_1 &= \frac{g_2(z_1, f(z_1)) - f'g_1(z_1, f(z_1))}{1 + cf'} \\ &\quad + \frac{f'' D_1 \nabla z_1 \cdot \nabla z_1}{1 + cf'} + \frac{\nabla \cdot (f'[D_2 - D_1] \nabla z_1)}{1 + cf'}, \end{aligned} \quad (23)$$

where  $f'' \equiv d^2 f(z_1)/dz_1^2$  is proportional to the manifold curvature and  $D_1 \nabla z_1 \cdot \nabla z_1$  is the scalar dissipation. Hence, in the model reaction–diffusion system, away from the boundaries,

$$\begin{aligned} z_2 &= f(z_1) + \epsilon \frac{g_2(z_1, f(z_1)) - f'g_1(z_1, f(z_1))}{1 + cf'} \\ &\quad + \epsilon \frac{\nabla \cdot (D_1 \nabla f(z_1)) - f' \nabla \cdot (D_1 \nabla z_1)}{1 + cf'} \\ &\quad + \epsilon \frac{\nabla \cdot ([D_2 - D_1] \nabla f(z_1))}{1 + cf'} + o(\epsilon) \\ &= f(z_1) + \epsilon \frac{g_2(z_1, f(z_1)) - f'g_1(z_1, f(z_1))}{1 + cf'} \\ &\quad + \epsilon \frac{f'' D_1 \nabla z_1 \cdot \nabla z_1}{1 + cf'} \\ &\quad + \epsilon \frac{\nabla \cdot (f'[D_2 - D_1] \nabla z_1)}{1 + cf'} + o(\epsilon). \end{aligned} \quad (24)$$

Close to the boundaries, this solution may have an error on the order of  $\epsilon$  if the boundary conditions are on the manifold. Otherwise the error close to the boundaries is on the order of one.

The following observations can be made from Eq. (24):

- In the reaction–diffusion inhomogeneous reactive systems, the compositions may be displaced from the slow manifold by an amount of order  $\epsilon$ . Each of the three terms in  $\epsilon$  may be nonzero even for  $c = 0$ .
- Three different mechanisms contribute to pulling compositions off the slow manifold, represented by the three terms in  $\epsilon$  in Eq. (24); in order, these are
  - (1) Noninvariance of the chemistry-based slow manifold;
  - (2) The combined effects of manifold curvature and scalar dissipation;
  - (3) Differential diffusion.

For zero diffusivities or homogeneous flows absent transport processes, the noninvariance effect is the only mechanism that pulls compositions off the slow manifold. If the slow manifold is invariant (i.e.,  $g_2 = f'g_1$  on the manifold), the noninvariance effect is zero. This is the advantage of using the invariant low-dimensional manifold to describe reactive flows. The latter two mechanisms are introduced by the diffusion process. The dissipation–curvature mechanism has previously been pointed out in Ref. [44], where the study is focused on systems with equal diffusivities. In Ref. [24], Ren et al. show the gross effects of diffusion processes without differentiating the dissipation–curvature and differential diffusion mechanisms.



- With equal diffusivities ( $D = D_1 = D_2$ ), and with  $L$  being the diffusion length scale, the perturbation caused by molecular diffusion is inversely proportional to the Damköhler number  $Da_f = \frac{L^2/D}{\varepsilon}$ , which is the ratio between the diffusion time scale and the fast chemical time scale. The larger the ratio, the less the composition is pulled off the slow manifold.

### 3.2. Evolution equation for the reduced composition variable

The evolution equation for  $z_1$  can be obtained by substituting Eq. (18) into the first equation of Eq. (13),

$$\begin{aligned} \frac{\partial z_1}{\partial t} &= g_1(z_1, f(z_1)) + \nabla \cdot (D_1 \nabla z_1) \\ &\quad + cf_1(z_1) + o(\varepsilon)/\varepsilon \\ &= g_1(z_1, f(z_1)) + \nabla \cdot (D_1 \nabla z_1) \\ &\quad + c \frac{g_2(z_1, f(z_1)) - f' g_1(z_1, f(z_1))}{1 + cf'} \\ &\quad + c \frac{f'' D_1 \nabla z_1 \cdot \nabla z_1}{1 + cf'} \\ &\quad + c \frac{\nabla \cdot (f' [D_2 - D_1] \nabla z_1)}{1 + cf'} + o(\varepsilon)/\varepsilon, \end{aligned} \quad (25)$$

where the second step follows from Eq. (23) and the remainder term  $o(\varepsilon)/\varepsilon$  approaches zero as  $\varepsilon$  tends to zero. As a comparison, by neglecting the “small” perturbation in Eq. (24), the first approximation gives the following evolution equation for  $z_1$ :

$$\frac{\partial z_1}{\partial t} = g_1(z_1, f(z_1)) + \nabla \cdot (D_1 \nabla z_1). \quad (26)$$

Equation (25) differs from Eq. (26) by the three additional terms. These three terms are in general nontrivial (even as  $\varepsilon$  tends to zero) and are referred to as noninvariance, dissipation–curvature, and differential diffusion, respectively. These terms arise, respectively, if the manifold is not invariant; if the manifold is curved and there is nonzero molecular diffusion; and if the diffusivities of the species differ. Hence the first-approximation approach to the reduced description is only accurate under some particular circumstances. One way to understand the origin of the extra terms is that due to the slight perturbation of composition (order of  $\mathcal{O}(\varepsilon)$ ; see Eq. (24)) caused by the noninvariance effect and molecular diffusion effects, the contribution from the fast chemistry to the evolution of the reduced composition variables may no longer be trivial. Hence when the slow manifolds are employed in the reduced description of inhomogeneous reactive systems, it is essential to be able to account for these effects.

As may be seen, in Eq. (25) one essential parameter is  $c$ , which describes the coupling between the

reduced composition variable  $z_1$  and the fast chemistry. If  $c$  is zero or  $\mathcal{O}(\varepsilon)$ , the noninvariance of the slow manifold and molecular diffusion have negligible effects on the evolution of the reduced composition, even though the full compositions are still off the slow manifold by the order of  $\varepsilon$  (see Eq. (24)). Here, we further explore the significance of the parameter  $c$ . For the model reaction–diffusion system considered (Eq. (13)), recall that the Jacobian matrix is

$$\mathbf{J} = \frac{1}{\varepsilon} \begin{bmatrix} -cf' & c \\ f' & -1 \end{bmatrix} + \mathcal{O}(1), \quad (27)$$

and the eigenvalue associated with the fast chemical time scale is  $-(1 + cf')/\varepsilon + \mathcal{O}(1)$ . Hence the corresponding fast eigenvector is

$$\mathbf{V}_f = \begin{bmatrix} -c \\ 1 \end{bmatrix} + \mathcal{O}(\varepsilon). \quad (28)$$

Recall that the represented subspace is spanned by  $\mathbf{B} = \begin{bmatrix} 1 \\ 0 \end{bmatrix}$  and the unrepresented subspace is spanned by  $\mathbf{U} = \begin{bmatrix} 0 \\ 1 \end{bmatrix}$ . Thus  $c$  is the tangent of the angle between  $\mathbf{V}_f$  and  $\mathbf{U}$ . Hence, in the reduced description of reactive flows, if the unrepresented subspace is not aligned with the fast directions (or the represented subspace is not perpendicular to the fast directions), a nontrivial coupling (e.g.,  $c$  in the model problem) between the reduced composition variables and the fast processes occurs and hence nontrivial extra terms arise in the evolution equation for the reduced composition variables (e.g., the last three extra terms in Eq. (25)).

### 3.3. Discussion

Given the evolution equation, Eq. (25), the reduced description of the unsteady reaction–diffusion system (Eq. (13)) is well posed given the appropriate boundary and initial conditions on  $z_1$ . In this study, the boundary and initial conditions for the reduced composition variable in the reduced description are taken directly from those corresponding conditions in the full description. This simplicity follows from the fact that, in this study, both the initial and boundary compositions are exactly on the chemistry-based slow manifold. When the ICE-PIC method [24] is used in the reduced description of reactive flows, the represented variables can be chosen so that the boundary and initial compositions are on the chemistry-based slow manifold.

When the boundary and initial compositions are not exactly on the chemistry-based slow manifold, thin boundary layers of compositions form close to the boundaries. Inside these boundary layers, the compositions are not within  $\mathcal{O}(\varepsilon)$  of the manifold, whereas far away from the boundaries, after the initial

transient, the compositions are close to the manifold. The evolution equation, Eq. (25), for the reduced composition variable is accurate to describe the long-term composition dynamics away from the boundaries. However, the boundary and initial conditions for the reduced description require a more thorough study [26,27], which is not undertaken in this paper.

For this model problem, Lam [26,27] has shown that results similar to Eq. (25) can be obtained via CSP.

### 3.4. Demonstration

To illustrate the different effects in Eq. (24) and Eq. (25), we consider a particular system in the class of Eq. (13),

$$\begin{aligned} \frac{\partial z_1}{\partial t} &= \frac{c}{\varepsilon} \left( z_2 - \frac{z_1}{1+az_1} \right) - dz_1 + \frac{\partial}{\partial x} \left( D_1 \frac{\partial z_1}{\partial x} \right), \\ \frac{\partial z_2}{\partial t} &= -\frac{1}{\varepsilon} \left( z_2 - \frac{z_1}{1+az_1} \right) - \frac{z_1}{(1+bz_1)^2} \\ &\quad + \frac{\partial}{\partial x} \left( D_2 \frac{\partial z_2}{\partial x} \right), \end{aligned} \quad (29)$$

where  $D_1$  and  $D_2$  are diffusion coefficients for  $z_1$  and  $z_2$ , respectively, with  $D_2 = D_1 + ex$ , with  $a, b, c, d, e$ , and  $D_1$  being specified constant model parameters. This system is an extension of the reactive models used by Davis and Skodjic [3] and Singh et al. [34]. Based on the reaction source term, a slow manifold is

$$\mathbf{z} = \begin{bmatrix} z_1 \\ z_2 \end{bmatrix} = \mathbf{z}^{\mathcal{M}}(z_1) = \begin{bmatrix} z_1 \\ \frac{z_1}{1+az_1} \end{bmatrix}. \quad (30)$$

In this study, the length of the physical domain is set to be  $L = 1$  over the physical domain  $0 \leq x \leq 1$ . The boundary conditions are on the manifold and given by

$$\begin{bmatrix} z_1(t, x = 0) \\ z_2(t, x = 0) \end{bmatrix} = \begin{bmatrix} 0 \\ 0 \end{bmatrix}$$

and

$$\begin{bmatrix} z_1(t, x = 1) \\ z_2(t, x = 1) \end{bmatrix} = \begin{bmatrix} 1 \\ \frac{1}{1+a} \end{bmatrix}.$$

Initially,  $z_1(t = 0, x)$  is linear in  $x$ , and  $z_2(t = 0, x)$  is determined from Eq. (30) so that the full compositions are initially on the slow manifold. Equation (29) is discretized in space with central finite differences over a mesh consisting of 101 equally spaced nodes and integrated in time using a stiff ODE integrator. Substantial efforts were made to ensure that the results are numerically accurate. Table 1 lists the four different cases designed. For the first three, we demonstrate the individual noninvariance, dissipation–curvature, and differential diffusion effects, respectively. The values used for  $D_1$  and  $\varepsilon$

Table 1  
Parameters for model systems, Eq. (29)

	Case 1	Case 2	Case 3	Case 4
$a$	0	1	0	1
$b$	1	1	0	1
$c$	1	1	1	1
$d$	2	1	1	2
$e$	0	0	3	3
$g_2 - f'g_1$	$\neq 0$	0	0	$\neq 0$
$f''$	0	$\neq 0$	0	$\neq 0$
$D_2 - D_1$	0	0	$\neq 0$	$\neq 0$

Note. The noninvariance, dissipation–curvature, and differential diffusion effects are proportional to  $g_2 - f'g_1$ ,  $f''$ , and  $D_2 - D_1$ , respectively. For the model systems considered,  $g_2 - f'g_1 = dz_1/(1+az_1)^2 - z_1/(1+bz_1)^2$ ,  $f'' = -2a/(1+az_1)^3$ , and  $D_2 - D_1 = ex$ .

are given in the figure legends (usually  $D_1 = 1$ ,  $\varepsilon = 0.01$ ).

The three terms in Eq. (24) giving  $\mathcal{O}(\varepsilon)$  departures from the manifold are proportional to  $g_2 - f'g_1$ ,  $f''$ , and  $D_2 - D_1$ , respectively. For the particular form of Eq. (29) these quantities are

$$\begin{aligned} g_2(z_1) - f'(z_1)g_1(z_1) &= \frac{dz_1}{(1+az_1)^2} - \frac{z_1}{(1+bz_1)^2}, \end{aligned} \quad (31)$$

$$f''(z_1) = \frac{-2a}{(1+az_1)^3}, \quad (32)$$

and

$$D_2 - D_1 = ex. \quad (33)$$

Note that these are identically zero for  $a = b, d = 1; a = 0$ ; and  $e = 0$ , respectively.

In Case 1, we demonstrate the noninvariance effect on composition and the reduced description. In Fig. 3, we compared the composition perturbations between the full model and the prediction from Eq. (24). As may be seen from the figure, the perturbation is of order  $\varepsilon$  as predicted. Away from the boundaries, after the initial transient ( $t \geq \mathcal{O}(\varepsilon)$ ), there is good agreement between the full model and the prediction. Close to the boundary, the perturbation predicted by Eq. (24) is significantly different from the full model due to the effect of the boundary conditions. As shown in Fig. 3, the extent of the boundary condition effect on composition decreases with  $\varepsilon$ . Fig. 4 shows the comparison of the evolution of  $z_1$  between the full model and the reduced description. As may be seen from the figure, the accuracy of the reduced description is substantially increased by incorporating the noninvariance effect in the reduced description. Even though the prediction for the composition perturbation is not accurate close to the boundary, the

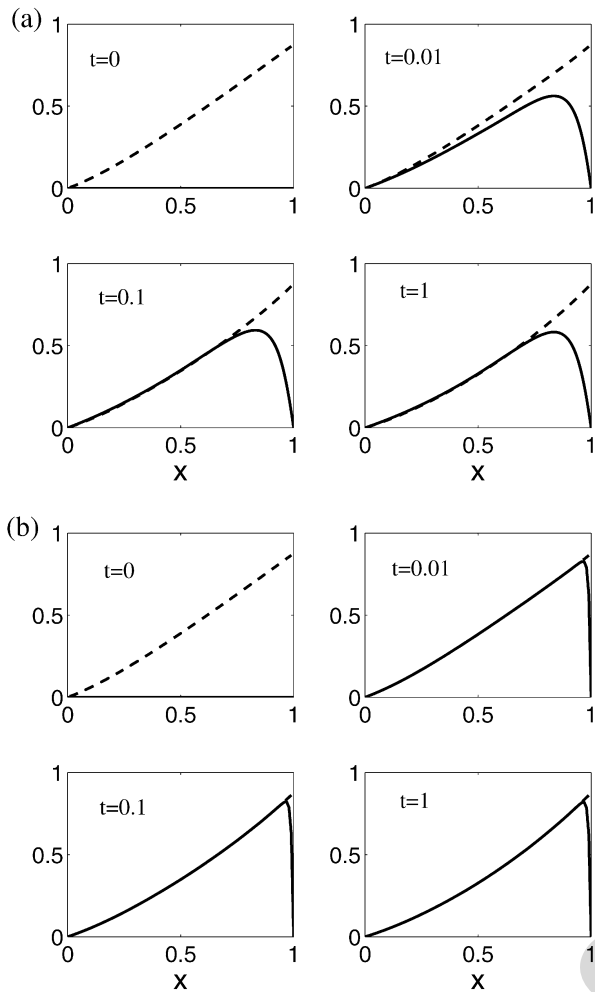


Fig. 3. Distribution of composition perturbation  $(z_2 - z_1)/(1 + az_1)/\varepsilon$  at different times for Case 1 in Table 1 with  $D_1 = 1$ . Solid line: full model (Eq. (29)); dashed line: prediction based on Eq. (24). (a)  $\varepsilon = 0.01$ ; (b)  $\varepsilon = 1 \times 10^{-4}$ .

prediction of the distribution of  $z_1$  shows good agreement with the full model over the whole physical domain.

In Case 2 and Case 3, we demonstrate the dissipation–curvature effect and the differential diffusion effect, respectively, on the composition and the reduced description, respectively. As may be seen from Figs. 5 and 6, both perturbations are order of  $\varepsilon$ . Away from the boundaries, after the initial transient ( $t \geq \mathcal{O}(\varepsilon)$ ), there is good agreement between the full model and the predictions. Also, as may be seen from Figs. 7 and 8, by incorporating the coupling, the accuracy of the reduced description is substantially improved. Most interestingly, as may be seen from Fig. 8, neglecting the differential diffusion effect in the reduced description gives a qualitatively inaccurate evolution of the reduced composition compared with the full model.

In Case 4, we consider the presence of all the three effects. As may be seen from Fig. 9, by taking into account the different effects, the accuracy of

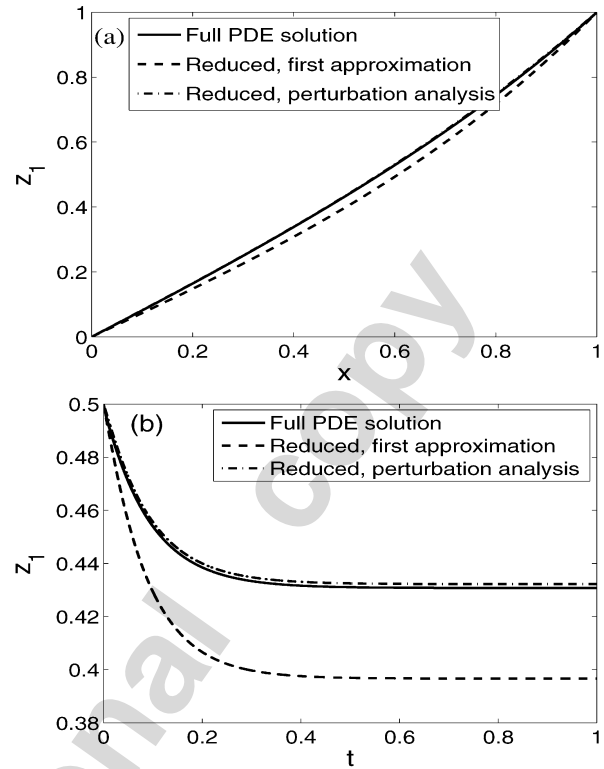


Fig. 4. Results for Case 1 in Table 1 with  $\varepsilon = 0.01$  and  $D_1 = 1$ . (a) Distribution of  $z_1$  at  $t = 1$ ; (b) evolution of  $z_1$  at  $x = \frac{1}{2}$ .

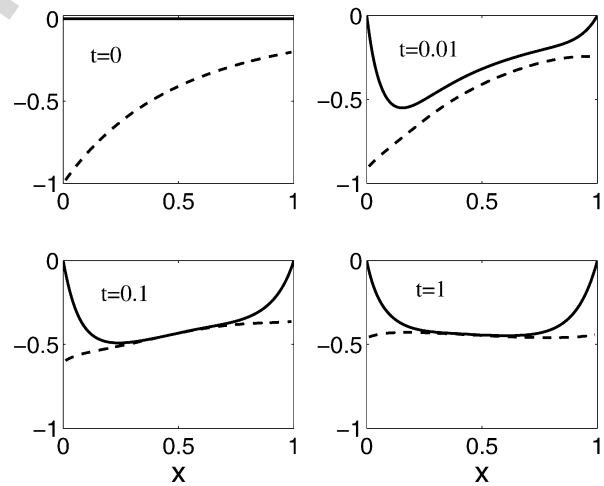


Fig. 5. Distribution of composition perturbation  $(z_2 - z_1)/(1 + az_1)$  at different times for Case 2 in Table 1 with  $\varepsilon = 0.01$  and  $D_1 = 1$ . Solid line: full model (Eq. (29)); dashed line: prediction based on Eq. (24).

the reduced description is substantially improved and moreover the accuracy increases with the decrease of  $\varepsilon$  as expected. In comparison, the error in the “first approximation” does not decrease with  $\varepsilon$ .

As pointed out in Section 3.1, the perturbation analysis is only valid when the fast chemical time scale is much smaller than the diffusion time scales, i.e.,  $L_1^2/(D_1\varepsilon) \gg 1$  and  $L_2^2/(D_2\varepsilon) \gg 1$  with  $L$  being the characteristic diffusion length scale. Also shown

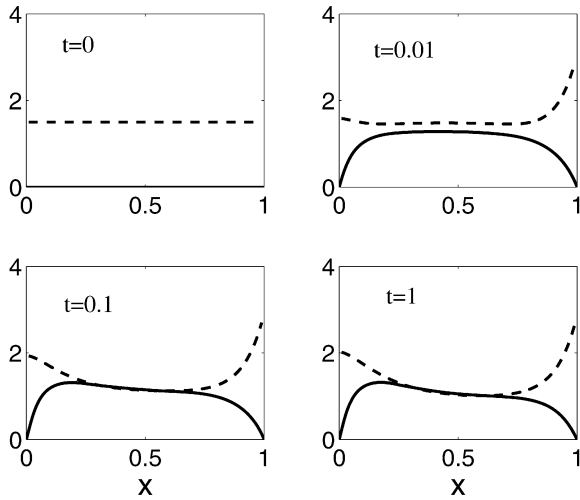


Fig. 6. Distribution of composition perturbation  $(z_2 - z_1 / (1 + az_1))$  at different times for Case 3 in Table 1 with  $\varepsilon = 0.01$  and  $D_1 = 1$ . Solid line: full model (Eq. (29)); dashed line: prediction based on Eq. (24).

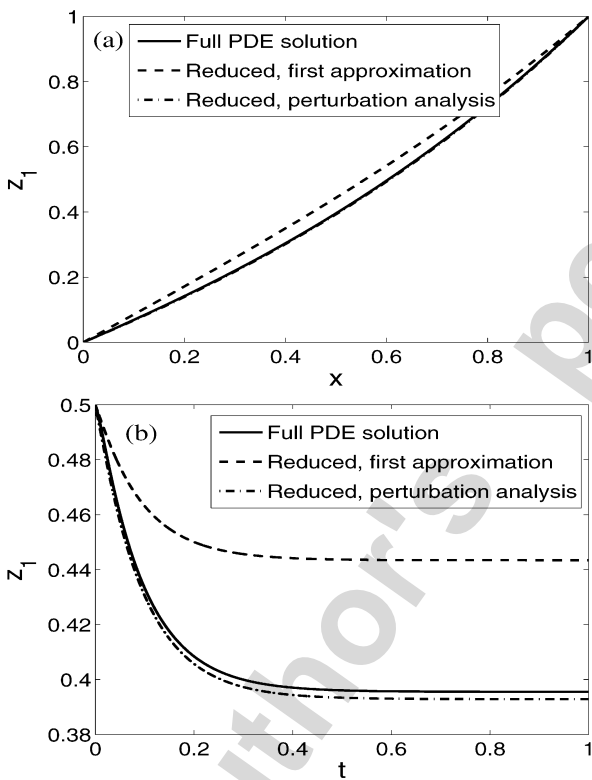


Fig. 7. Results for Case 2 in Table 1 with  $\varepsilon = 0.01$  and  $D_1 = 1$ . (a) Distribution of  $z_1$  at  $t = 1$ ; (b) evolution of  $z_1$  at  $x = \frac{1}{2}$ .

in Fig. 10, when the diffusion time scale is comparable to the fast time scale, even the prediction from Eq. (25) (taking into account all the three effects) results in large errors. The reason for this particular case, as demonstrated in Fig. 11, is that the molecular diffusion pulls the composition far away from the slow manifold. As expected, the coupling obtained based on small perturbation analysis is not accurate.

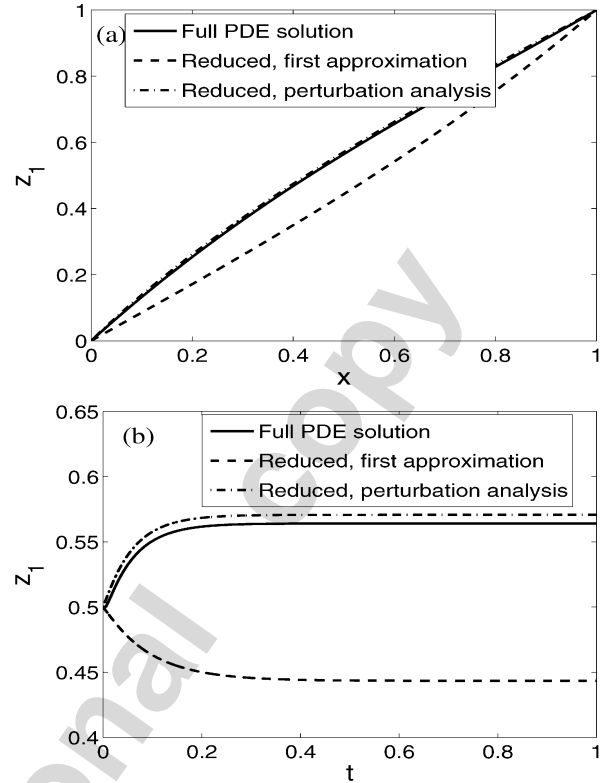


Fig. 8. Results for Case 3 in Table 1 with  $\varepsilon = 0.01$  and  $D_1 = 1$ . (a) Distribution of  $z_1$  at  $t = 1$ ; (b) evolution of  $z_1$  at  $x = \frac{1}{2}$ .

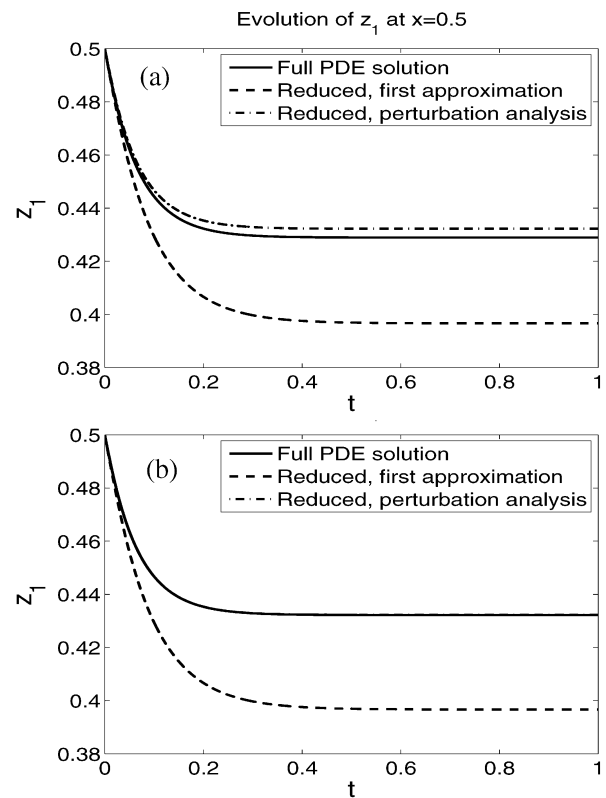


Fig. 9. Evolution of  $z_1$  at  $x = 0.5$  for Case 4 in Table 1 with  $D_1 = 1$ . (a)  $\varepsilon = 0.01$ ; (b)  $\varepsilon = 1 \times 10^{-4}$ . On (b), the difference between the full PDE solution and the reduced description by perturbation analysis is indistinguishable.



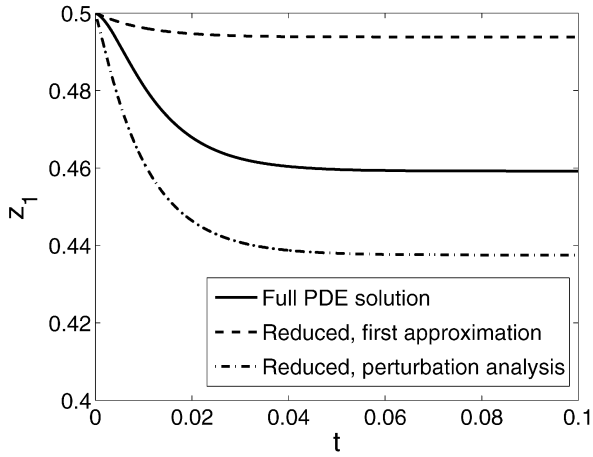


Fig. 10. The evolution of  $z_1$  at  $x = 0.5$  for Case 2 in Table 1 with  $\varepsilon = 0.01$  and  $D_1 = 10$ .

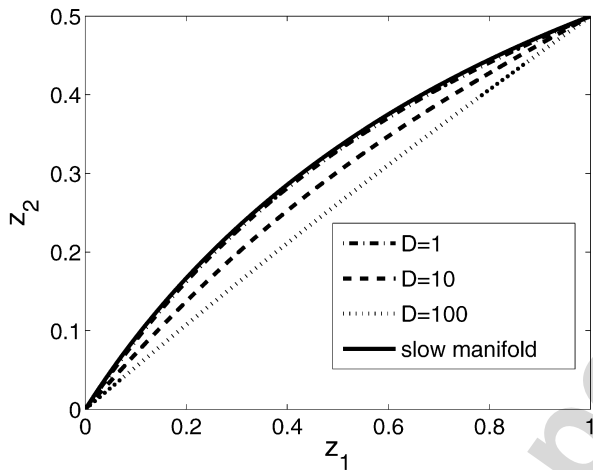


Fig. 11. Steady-state distribution of compositions in the composition space obtained from Case 2 in Table 1 with  $\varepsilon = 0.01$  and different values of diffusivity  $D$  ( $= D_1 = D_2$ ).

For this regime, the use of chemistry-based slow manifolds to describe inhomogeneous reactive flow is inadequate.

#### 4. Close-parallel assumption for reduced description of reactive flows

The close-parallel assumption was first employed by Tang and Pope [47] to provide a more accurate projection for homogeneous systems in the rate-controlled constrained equilibrium method [14,15]. In Ref. [24], the close-parallel assumption is extended by Ren et al. to incorporate the transport–chemistry coupling in the reduced description of reactive flows. In that study, the chemistry-based low-dimensional manifold used is invariant and therefore the noninvariance effect is zero. Although in Ref. [24] no justification for the close-parallel assumption was presented, as reported, when the transport–chemistry coupling is

incorporated, the accuracy of the reduced description of the reactive systems is substantially improved.

In the following, we extend the assumption to the general case where the chemistry-based low-dimensional manifold is not necessarily invariant. In model reaction–diffusion systems, for the first time, we demonstrate the close-parallel phenomena from different aspects and provide support for the assumption. We show that the close-parallel assumption gives the same evolution equation for the reduced composition variable as the perturbation analysis. Finally we discuss the noninvariance effect and transport–chemistry coupling in the reduced description of a general reactive flow.

##### 4.1. An overview of the close-parallel assumption

In the reduced description of an inhomogeneous reactive flow, the system is described in terms of the reduced composition variables  $\mathbf{r}$ . In the close-parallel assumption, the compositions are assumed to lie on a low-dimensional manifold which is close to and parallel to the chemistry-based slow manifold (see Fig. 1). In other words, in the inhomogeneous flow, the full system evolves on a manifold which is close to and parallel to the chemistry-based slow manifold employed. The assumption is expected to be valid in the regime where fast chemical time scales are smaller than the transport time scales, such as diffusion time scales. In this regime, as shown below, with the use of the close-parallel assumption, the reduced description agrees well with the full reactive system.

Recall that the compositions can be expressed as  $\mathbf{z}(\mathbf{x}, t) = \mathbf{z}^{\mathcal{M}}(\mathbf{r}(\mathbf{x}, t)) + \delta\mathbf{z}(\mathbf{x}, t)$  with  $\delta\mathbf{z} = \mathbf{U}\delta\mathbf{u}$  (Eqs. (6), (7)), and substituting Eqs. (6) and (7) into Eq. (10), we obtain

$$\frac{\partial \mathbf{r}}{\partial t} + v_i \frac{\partial \mathbf{r}}{\partial x_i} = \mathbf{B}^T \mathbf{D} \{ \mathbf{z}^{\mathcal{M}}(\mathbf{r}) + \mathbf{U}\delta\mathbf{u} \} + \mathbf{B}^T \mathbf{S}(\mathbf{z}^{\mathcal{M}}(\mathbf{r}) + \mathbf{U}\delta\mathbf{u}). \quad (34)$$

For the first term on the right-hand side, since  $\mathbf{D}$  depends on derivatives of  $\mathbf{z}$ , and since by assumption  $\mathbf{z}$  is close to and parallel to  $\mathbf{z}^{\mathcal{M}}$ , the diffusion process is not sensitive to the perturbations and the indicated approximation is

$$\mathbf{B}^T \mathbf{D} \{ \mathbf{z}^{\mathcal{M}}(\mathbf{r}) + \mathbf{U}\delta\mathbf{u} \} \approx \mathbf{B}^T \mathbf{D} \{ \mathbf{z}^{\mathcal{M}}(\mathbf{r}) \}. \quad (35)$$

For chemical reaction, however, small perturbations off the manifold may result in significant changes in the reaction rate due to fast processes in the chemical kinetics. The assumption that  $\mathbf{z}$  is close to  $\mathbf{z}^{\mathcal{M}}$  implies  $\delta\mathbf{z}$  (or  $\mathbf{U}\delta\mathbf{u}$ ) is small, and hence the last term on the right-hand side of Eq. (34) can be well approximated by

$$\mathbf{B}^T \mathbf{S}(\mathbf{z}^{\mathcal{M}}(\mathbf{r}) + \mathbf{U}\delta\mathbf{u}) \approx \mathbf{B}^T \mathbf{S}(\mathbf{z}^{\mathcal{M}}) + \mathbf{B}^T \mathbf{J} \mathbf{U} \delta\mathbf{u}, \quad (36)$$

where  $J_{ij} \equiv \frac{\partial S_i}{\partial z_j} \Big|_{\mathbf{z}=\mathbf{z}^{\mathcal{M}}}$  is the Jacobian matrix. Hence, with the close-parallel assumption, we obtain

$$\frac{\partial \mathbf{r}}{\partial t} + v_i \frac{\partial \mathbf{r}}{\partial x_i} = \mathbf{B}^T \mathbf{D}\{\mathbf{z}^{\mathcal{M}}(\mathbf{r})\} + \mathbf{B}^T \mathbf{S}(\mathbf{z}^{\mathcal{M}}(\mathbf{r})) + \mathbf{B}^T \mathbf{J} \mathbf{U} \delta \mathbf{u}. \quad (37)$$

The perturbation  $\delta \mathbf{z}$  ( $= \mathbf{U} \delta \mathbf{u}$ ) can be obtained by considering the balance equation in the normal subspace of the manifold and therefore an accurate evolution equation can be deduced for the reduced composition variables. For given  $\mathbf{r}$ , we denote by  $\mathbf{T}(\mathbf{r})$  an  $n_s \times n_r$  orthogonal matrix spanning the tangent subspace of the manifold at  $\mathbf{z}^{\mathcal{M}}(\mathbf{r})$ , and similarly  $\mathbf{N}(\mathbf{r})$  is an  $n_s \times n_u$  orthogonal matrix spanning the normal subspace. Hence,  $\mathbf{N}^T \mathbf{T} = \mathbf{0}$ ,  $\mathbf{N}^T \mathbf{N} = \mathbf{I}_{n_u \times n_u}$ ,  $\mathbf{T}^T \mathbf{T} = \mathbf{I}_{n_r \times n_r}$ , and  $\mathbf{N} \mathbf{N}^T + \mathbf{T} \mathbf{T}^T = \mathbf{I}_{n_s \times n_s}$ . For the model problems, as shown below, the tangent and normal subspaces are readily known. For realistic reactive flows, when using the ICE-PIC method in the reduced description, the tangent and normal subspaces of the chemistry-based manifold are readily computed [24, 53]. For the ILDM method, as shown in Ref. [43], good approximations to the tangent and normal subspace are provided by the slow and fast subspaces identified in the ILDM method.

Considering the balance of the governing PDEs (Eq. (1)) in the normal subspace, with  $\mathbf{z} = \mathbf{z}^{\mathcal{M}} + \delta \mathbf{z}$ , we have

$$\begin{aligned} \mathbf{N}^T(\mathbf{r}) \frac{\partial (\mathbf{z}^{\mathcal{M}} + \delta \mathbf{z})}{\partial t} + \mathbf{N}^T(\mathbf{r}) v_i \frac{\partial (\mathbf{z}^{\mathcal{M}} + \delta \mathbf{z})}{\partial x_i} \\ = \mathbf{N}^T(\mathbf{r}) \mathbf{D}\{\mathbf{z}^{\mathcal{M}} + \delta \mathbf{z}\} + \mathbf{N}^T(\mathbf{r}) \mathbf{S}(\mathbf{z}^{\mathcal{M}} + \delta \mathbf{z}). \end{aligned} \quad (38)$$

The close-parallel assumption amounts to the approximations

$$\mathbf{N}^T(\mathbf{r}) \frac{\partial \delta \mathbf{z}}{\partial t} \approx 0 \quad (39)$$

and

$$\mathbf{N}^T(\mathbf{r}) v_i \frac{\partial \delta \mathbf{z}}{\partial x_i} \approx 0. \quad (40)$$

(Note that  $\mathbf{N}^T \frac{\partial \mathbf{z}^{\mathcal{M}}}{\partial t}$  and  $\mathbf{N}^T v_i \frac{\partial \mathbf{z}^{\mathcal{M}}}{\partial x_i}$  are exactly zero.) Hence Eq. (38) can be simplified to

$$0 \approx \mathbf{N}^T(\mathbf{r}) \mathbf{D}\{\mathbf{z}^{\mathcal{M}} + \delta \mathbf{z}\} + \mathbf{N}^T(\mathbf{r}) \mathbf{S}(\mathbf{z}^{\mathcal{M}} + \delta \mathbf{z}). \quad (41)$$

Note that the terms on the right-hand side of Eq. (41) are the components of molecular diffusion and chemical reactions in the normal subspace, respectively. Equation (41) implies that in the normal subspace of the manifold, there is a balance between the molecular diffusion and reaction. (When the transport processes are absent, the system evolves on a low-dimensional manifold that is close and parallel to the slow manifold and Eq. (41) implies that the reaction rate in the

normal subspace of the manifold is negligible compared to the reaction rate in the tangent subspace.) It is worthwhile to make a comparison between Eq. (41) and the analogous equations obtained in the reduced description by the CSP method [22,23,25,28,29], the ILDM method [41–43], and the ASIM method [34]. In the reduced description by the CSP method, after the relaxation of fast time scales, there exists a balance between transport processes and reaction in the fast subspace which is constructed by the refined CSP basis. Similarly, in the ILDM and ASIM methods, there exists a balance between transport processes and reaction in the fast subspace which is identified based on the local Jacobian matrix. For the model problems considered in Eq. (13), it is easy to show that these relations from CSP, ILDM, ASIM, and the close-parallel assumption are identical (to leading order) [27,43]. However, the functionality of these equations in the reduced descriptions by the different approaches is different. In the CSP and ASIM methods, the differential (or differential algebraic) equations define the slow manifolds for inhomogeneous flows, whereas, in the close-parallel assumption, Eq. (41) is used (as shown below) to obtain the composition perturbations off the chemistry-based slow manifolds. Another point worthy of mention is that, for the general case, the basis  $\mathbf{N}$  used in the close-parallel approach is different from the analogous bases used in the other approaches, and in particular  $\mathbf{N}$  is continuous if the chemistry-based manifold is sufficient smooth, whereas the fast subspace constructed in CSP, ILDM, and ASIM may be discontinuous.

Since  $\mathbf{D}$  depends on the derivative of  $\mathbf{z}(\mathbf{x}, t)$  and since by assumption  $\mathbf{z}(\mathbf{x}, t)$  is close and parallel to  $\mathbf{z}^{\mathcal{M}}(\mathbf{r}(\mathbf{x}, t))$ , Eq. (41) can be simplified as

$$0 \approx \mathbf{N}^T \mathbf{D}\{\mathbf{z}^{\mathcal{M}}\} + \mathbf{N}^T \mathbf{S}(\mathbf{z}^{\mathcal{M}}) + \mathbf{N}^T \mathbf{J}(\mathbf{z}^{\mathcal{M}}) \delta \mathbf{z}, \quad (42)$$

where  $\delta \mathbf{z} = \mathbf{U} \delta \mathbf{u}$ . In Eq. (42), if the slow manifold used is invariant, then  $\mathbf{N}^T \mathbf{S}(\mathbf{z}^{\mathcal{M}})$  is zero. In [24], the study is focused on the use of invariant manifolds. Here we extend to the general case.

By manipulating Eq. (42), we obtain

$$\begin{aligned} \delta \mathbf{u} = -(\mathbf{N}^T \mathbf{J}(\mathbf{z}^{\mathcal{M}}) \mathbf{U})^{-1} \\ \times [\mathbf{N}^T \mathbf{D}\{\mathbf{z}^{\mathcal{M}}\} + \mathbf{N}^T \mathbf{S}(\mathbf{z}^{\mathcal{M}})]. \end{aligned} \quad (43)$$

As may be seen from Eq. (43), based on the close-parallel assumption, the compositions in the inhomogeneous reactive flows are pulled off the slow manifold due to the molecular diffusion and the noninvariance of the slow manifold.

Substituting Eq. (43) into Eq. (37), we have the evolution equations for the reduced composition vari-

able  $\mathbf{r}$ ,

$$\frac{\partial \mathbf{r}}{\partial t} + v_i \frac{\partial \mathbf{r}}{\partial x_i} = \mathbf{B}^T \mathbf{D} \{ \mathbf{z}^{\mathcal{M}}(\mathbf{r}) \} + \mathbf{B}^T \mathbf{S}(\mathbf{z}^{\mathcal{M}}(\mathbf{r})) + \mathbf{H}^T \mathbf{S}(\mathbf{z}^{\mathcal{M}}) + \mathbf{H}^T \mathbf{D} \{ \mathbf{z}^{\mathcal{M}} \}, \quad (44)$$

where  $\mathbf{H}^T \equiv -\mathbf{B}^T \mathbf{J} \mathbf{U} (\mathbf{N}^T \mathbf{J} \mathbf{U})^{-1} \mathbf{N}^T$  is an  $n_r \times n_s$  matrix. Compared to the first approximation (Eq. (12)), there are two extra terms that arise from the noninvariance effect and diffusion–chemistry coupling.

Hence, as shown in Eqs. (43) and (44), the compositions in general inhomogeneous reactive flows are pulled off the chemistry-based slow manifold by the noninvariance of manifold and molecular diffusion, and correspondingly, these perturbations introduce coupling terms into the evolution equation of the reduced composition variables.

#### 4.2. Noninvariance effect and transport–chemistry coupling in general reactive flows

For the general reactive flow, we further explore Eq. (44) and explicitly show the dissipation–curvature effect and the differential diffusion effect on the reduced description of reactive flows. In describing combustion processes, the diffusion model, Eq. (2), is widely used. We consider the decomposition of the diagonal diffusivity matrix  $\mathbf{\Gamma}$  as

$$\mathbf{\Gamma} = \bar{\Gamma} \mathbf{I} + \delta \mathbf{\Gamma}, \quad (45)$$

where  $\bar{\Gamma}$  is a reference diffusivity, chosen to make  $\delta \mathbf{\Gamma}$  small in some sense. A natural choice of  $\bar{\Gamma}$  is the species-weighted diffusivity  $\| \mathbf{\Gamma} \mathbf{z}^{\mathcal{M}} \| / \| \mathbf{z}^{\mathcal{M}} \|$ .

Substituting Eqs. (2) and (45) into (44), we have

$$\begin{aligned} \frac{\partial \mathbf{r}}{\partial t} + v_i \frac{\partial \mathbf{r}}{\partial x_i} &= \mathbf{B}^T \mathbf{D} \{ \mathbf{z}^{\mathcal{M}}(\mathbf{r}) \} + \mathbf{B}^T \mathbf{S}(\mathbf{z}^{\mathcal{M}}(\mathbf{r})) \\ &+ \mathbf{H}^T \mathbf{S}(\mathbf{z}^{\mathcal{M}}) + \mathbf{H}^T \frac{\partial^2 \mathbf{z}^{\mathcal{M}}}{\partial r_j \partial r_k} \left( \bar{\Gamma} \frac{\partial r_j}{\partial x_i} \frac{\partial r_k}{\partial x_i} \right) \\ &+ \mathbf{H}^T \frac{1}{\rho} \nabla \cdot (\rho \delta \mathbf{\Gamma} \nabla \mathbf{z}^{\mathcal{M}}), \end{aligned} \quad (46)$$

where  $\mathbf{H}^T = -\mathbf{B}^T \mathbf{J} \mathbf{U} (\mathbf{N}^T \mathbf{J} \mathbf{U})^{-1} \mathbf{N}^T$ . Hence, as demonstrated in the reaction–diffusion system, in general reactive flows, the transport processes introduce two usually nontrivial coupling terms into the reduced composition evolution equation: one is due to the combination of scalar dissipation and manifold curvature, the other to differential diffusion. These two terms represent the transport–chemistry coupling. Notice that the decomposition of  $\mathbf{H}^T \mathbf{D}$  into these two terms is not unique. Different decompositions of  $\mathbf{\Gamma}$  may lead to different decompositions of  $\mathbf{H}^T \mathbf{D}$ .

One essential quantity in Eq. (46) is the matrix  $\mathbf{H}^T$  which provides the coupling information between the reduced composition and chemistry. (It plays the

same role as the parameter  $c$  in the model reaction.) Assume that the Jacobian can be decomposed as

$$\mathbf{J} = \mathbf{V} \mathbf{\Lambda} \tilde{\mathbf{V}} = [\mathbf{V}_s \quad \mathbf{V}_f] \mathbf{\Lambda} \begin{bmatrix} \tilde{\mathbf{V}}_s \\ \tilde{\mathbf{V}}_f \end{bmatrix}, \quad (47)$$

where  $\mathbf{V}$  is the  $n_s \times n_s$  right eigenvector matrix and  $\tilde{\mathbf{V}} = \mathbf{V}^{-1}$  is the left eigenvector matrix. The diagonal matrix  $\mathbf{\Lambda}$ , of dimension  $n_s \times n_s$ , contains the eigenvalues of  $\mathbf{J}$ , ordered in decreasing value of their real parts. The columns of  $\mathbf{V}_s$  ( $n_s \times n_r$ ) span the slow subspace, and the columns of  $\mathbf{V}_f$  ( $n_s \times n_u$ ) span the fast subspace. It is easy to verify that if the unrepresented subspace  $\text{span}(\mathbf{U})$  is aligned with the fast subspace (i.e., the represented subspace  $\text{span}(\mathbf{B})$  is perpendicular to the fast subspace),  $\mathbf{H}^T$  is zero; otherwise a nontrivial coupling between the reduced composition variables and chemistry may occur and hence nontrivial extra terms may arise in the evolution equation for the reduced composition variables (e.g., the last three extra terms in Eq. (46)).

As may be seen from Eq. (46), the “first approximation” for the evolution equation for the reduced composition variables is only accurate under the special circumstances: negligible noninvariance effect and negligible transport–chemistry coupling. One way to reduce the noninvariance effect and the transport–chemistry coupling is to carefully choose the represented subspace so that it is perpendicular to the fast directions. Since the fast directions  $\mathbf{V}_f$  vary with position in composition space, for a fixed reduced representation with constant  $\mathbf{B}$ , the best that can practically be achieved is a choice of  $\mathbf{B}$  that minimizes the principal angles between  $\text{span}(\mathbf{B})$  and  $\text{span}(\mathbf{V}_f)$  for compositions in the region of the slow manifold where the transport–chemistry coupling is significant. Two other effective ways to increase the accuracy of the “first approximation” are to use invariant manifolds in the reduced description, and to increase the dimensionality of the reduced description (i.e., increase the number of reduced composition variables). When invariant manifolds are used in the reduced description, the noninvariance effect is zero. By increasing the dimensionality of the reduced description, the transport–chemistry coupling is likely to decrease due to the decrease of both manifold curvature and the possible differential diffusion effect. At the same level of reduction, accounting for the noninvariant effect and the transport coupling usually gives a more accurate description. As reported in Ref. [24], when using the ICE-PIC approach to perform the species reconstruction for one-dimensional premixed laminar flames of methane/air mixture, with transport–chemistry coupling, the ICE-PIC method with 8 reduced composition variables is much more accurate than the one with the same reduced composition but without transport–chemistry coupling; more-

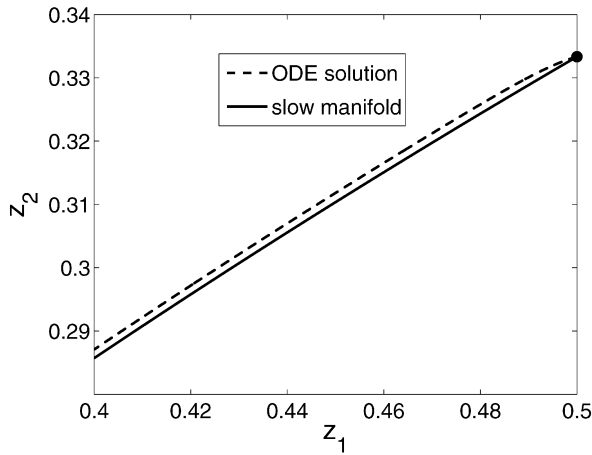


Fig. 12. The reaction trajectory from Eq. (48) with  $\varepsilon = 0.01$  starting from the initial condition  $[\frac{1}{2}; \frac{1}{3}]$  in the composition space  $z_1$ – $z_2$ . The small parameter  $\varepsilon = 0.01$ .

over it achieves comparable accurate results with the one with 12 reduced composition variables that does not include the coupling.

#### 4.3. Validation in the reaction–diffusion systems

The close-parallel phenomena are observed in both homogeneous and inhomogeneous systems, which serve as supports for the close-parallel assumption. Fig. 12 shows the reaction trajectory in the composition space for the homogeneous reactive system (with  $\varepsilon = 0.01$ ),

$$\begin{aligned} \frac{dz_1}{dt} &= \frac{1}{\varepsilon} \left( z_2 - \frac{z_1}{1+z_1} \right) - 2z_1, \\ \frac{dz_2}{dt} &= -\frac{1}{\varepsilon} \left( z_2 - \frac{z_1}{1+z_1} \right) - \frac{z_1}{(1+z_1)^2}. \end{aligned} \quad (48)$$

The initial composition  $[\frac{1}{2}; \frac{1}{3}]$  is on the slow manifold

$$\mathbf{z} = \mathbf{z}^{\mathcal{M}}(z_1) = \begin{bmatrix} z_1 \\ \frac{z_1}{1+z_1} \end{bmatrix}.$$

As may be seen from the figure, due to the noninvariance of the slow manifold, the reaction trajectory is pulled off the slow manifold in the initial transient. After that the reaction trajectory is close to and parallel to the slow manifold.

Fig. 13a shows the evolution of the compositions at four different physical locations in the composition space for Case 2 in Table 1 with  $\varepsilon = 0.1$  and  $D_1 = 1$ . Due to molecular diffusion, in the initial transient, all the compositions are pulled off the chemistry-based slow manifold (invariant in this case). After the initial transient, the compositions at different physical locations evolve approximately in the same manifold, close to and parallel to the slow invariant manifold. (This parallel phenomena is also observed by Goussis et al. [29] in studying the diffusion and chemical

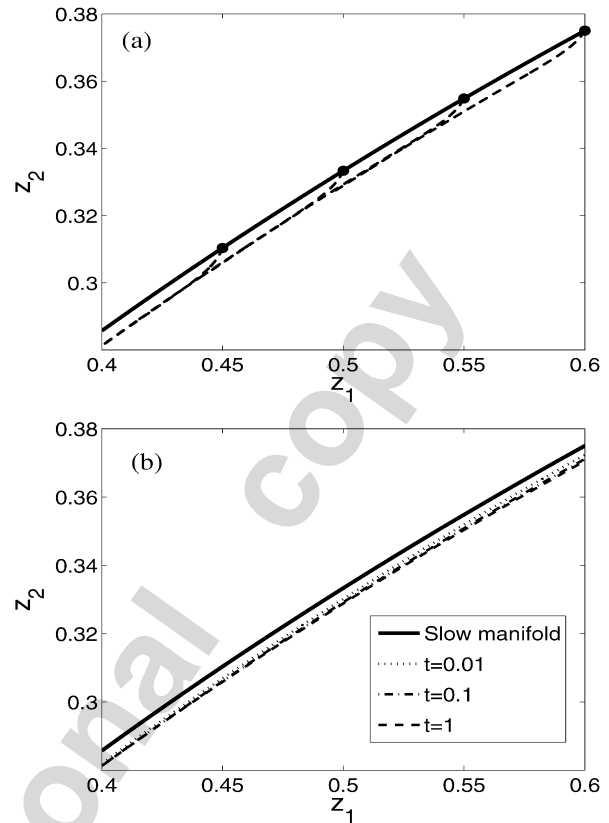


Fig. 13. Results for Case 2 in Table 1 with  $\varepsilon = 0.01$  and  $D_1 = 1$ . (a) Evolution of compositions at four different physical locations in the composition space. Solid line: slow manifold; solid dots: initial compositions; dashed lines: evolution trajectories. (b) The distribution of the compositions at different times in the composition space.

time scales.) Another perspective to look at this close-parallel phenomena is to study the composition distribution in the composition space at discrete times. As may be seen from Fig. 13b, in the composition space, during the evolution, the compositions in the physical domain stay close to the slow manifold. A close look reveals that after the initial transient, at each discrete time, the compositions in the physical domain approximately lie on a manifold that is close to and parallel to the slow manifold.

As discussed in Section 4.1, the close-parallel assumption implies a balance between the molecular diffusion and reaction process in the normal subspace of the slow manifold (see Eq. (41)). We demonstrate this balance in Fig. 14. The figure shows the components of the rate of change, molecular diffusion, and reaction in the normal subspace of the manifold for Case 4 in Table 1 with  $\varepsilon = 0.01$  and  $D_1 = 1$ . As may be seen, after the initial transient ( $\approx 0.01$  s), the dominant balance is between reaction and molecular diffusion over the whole physical domain.

Besides the above phenomenological validation, it is easy to show that for the class of reaction–diffusion systems (Eq. (13)) considered in Section 3,



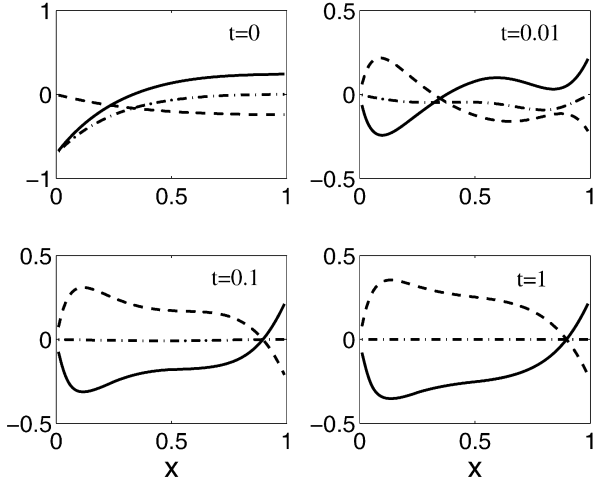


Fig. 14. The balance of rate of change, molecular diffusion, and reaction in the normal subspace of the slow manifold for Case 4 in Table 1 with  $\varepsilon = 0.01$  and  $D_1 = 1$ . Solid line: molecular diffusion; dashed line: reaction; dash-dotted line: rate of change.

the close-parallel assumption gives the same evolution equation for the reduced composition variable as the perturbation analysis. Recall that the represented subspace is  $\mathbf{B} = \begin{bmatrix} 1 \\ 0 \end{bmatrix}$ , the unrepresented subspace is  $\mathbf{U} = \begin{bmatrix} 0 \\ 1 \end{bmatrix}$ , the tangent unit vector of the slow manifold is  $\mathbf{T} = \frac{1}{\sqrt{1+f'^2}} \begin{bmatrix} 1 \\ f'(z_1) \end{bmatrix}$ , and the normal unit vector is  $\mathbf{N} = \frac{1}{\sqrt{1+f'^2}} \begin{bmatrix} -f'(z_1) \\ 1 \end{bmatrix}$ . The Jacobian matrix on the slow manifold is

$$\mathbf{J}(\mathbf{z}^{\mathcal{M}}) = \begin{bmatrix} -\frac{cf'}{\varepsilon} + \nabla_{z_1} g_1 & \frac{c}{\varepsilon} + \nabla_{z_2} g_1 \\ \frac{f'}{\varepsilon} + \nabla_{z_1} g_2 & -\frac{1}{\varepsilon} + \nabla_{z_2} g_2 \end{bmatrix}_{\mathbf{z}=\mathbf{z}^{\mathcal{M}}}, \quad (49)$$

where  $\nabla_{z_1}$  and  $\nabla_{z_2}$  are partial derivative operators with respect to  $z_1$  and  $z_2$ , respectively. Substituting the above expressions into Eq. (43), we obtain

$$\begin{aligned} \delta \mathbf{u} &= \delta u \\ &= \frac{g_2(z_1, f(z_1)) - f' g_1(z_1, f(z_1))}{\frac{1}{\varepsilon}(1 + cf') + \nabla_{z_2} g_1 f' - \nabla_{z_2} g_2} \\ &\quad - \frac{f' \nabla \cdot (D_1 \nabla z_1) - \nabla \cdot (D_2 \nabla z_2)}{\frac{1}{\varepsilon}(1 + cf') + \nabla_{z_2} g_1 f' - \nabla_{z_2} g_2} \\ &= \varepsilon \frac{g_2(z_1, f(z_1)) - f' g_1(z_1, f(z_1))}{1 + cf'} \\ &\quad + \varepsilon \frac{f'' D_1 \nabla z_1 \cdot \nabla z_1}{1 + cf'} \\ &\quad + \varepsilon \frac{\nabla \cdot (f' [D_2 - D_1] \nabla z_1)}{1 + cf'} + \mathcal{O}(\varepsilon^2). \quad (50) \end{aligned}$$

Hence for the reaction–diffusion systems, the close-parallel assumption predicts  $z_2 = f(z_1) + \delta u$ , which

is identical to Eq. (24) (to leading order). By substituting Eq. (50) into Eq. (37), it is easy to verify that the evolution equation for  $z_1$  given by the close-parallel assumption is identical to Eq. (25) (to leading order).

#### 4.4. Effect of convection on the composition and the reduced description

Besides the diffusion and reaction, most inhomogeneous flows involve convection. It is important to understand its effect and role in the reduced description. As mentioned [42,44], convection alone does not pull compositions off chemistry-based manifolds and in fact it does not even change the composition of a fluid particle. Moreover in the reduced description (see Eq. (10)), the corresponding convection term for the reduced composition is exact, with no approximation needed.

However, in spite of its seeming insignificance, convection does have significant effects both on the composition and the reduced description. Convection manifests its effect through the diffusion process by changing the gradients of the composition field. It is well known that convection may introduce small flow structures such as eddies and therefore changes the length and time scales of diffusion. The compositions in a reactive flow may be further pulled off the chemistry-based manifold by enhanced diffusion caused by convection. In a regime where convection is not so strong that the time scales of the enhanced diffusion are still much larger than the fast chemical time scales, the compositions still lie close to the chemistry-based slow manifold. This is true when the convection time scales are much larger than the fast chemical time scales. As shown below, in this regime, the close-parallel assumption for the reduced description, Eq. (44), and its implication, Eq. (41), are still valid. When convection is so strong that the time scales of the enhanced diffusion are comparable to or smaller than the fast chemical time scales, the compositions are pulled far away from the chemistry-based slow manifold. As expected the transport–chemistry coupling obtained based on small perturbation is not accurate. Consequently, the close-parallel assumption for the reduced description, Eq. (44), and its implication, Eq. (41), are not accurate in these circumstances. This occurs when the convection time scales are comparable to or smaller than the fast chemical time scales.

To illustrate the effect of convection, we add convection to the model system, Eq. (29), so that the governing equations are

$$\begin{aligned} \frac{\partial z_1}{\partial t} + v \frac{\partial z_1}{\partial x} &= \frac{c}{\varepsilon} \left( z_2 - \frac{z_1}{1 + az_1} \right) \\ &\quad - dz_1 + \frac{\partial}{\partial x} \left( D_1 \frac{\partial z_1}{\partial x} \right), \end{aligned}$$

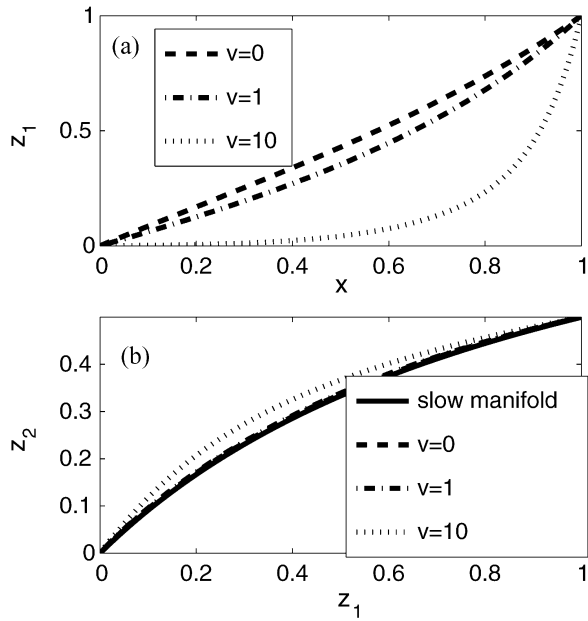


Fig. 15. Results from the system Eq. (51) with different values of velocity. All the other parameters including boundary and initial conditions are the same as those for Case 4 of the system Eq. (29) in Table 1 with  $\varepsilon = 0.01$  and  $D_1 = 1$ . (a) Distribution of  $z_1$  at  $t = 1$  for different velocities. (b) Steady-state distribution of compositions in the composition space.

$$\frac{\partial z_2}{\partial t} + v \frac{\partial z_2}{\partial x} = -\frac{1}{\varepsilon} \left( z_2 - \frac{z_1}{1 + az_1} \right) - \frac{z_1}{(1 + bz_1)^2} + \frac{\partial}{\partial x} \left( D_2 \frac{\partial z_2}{\partial x} \right), \quad (51)$$

where  $v$  is the velocity, and all the other parameters including boundary and initial conditions are the same as those specified in Eq. (29). For simplicity, the velocity is taken to be constant and uniform over the whole domain. As may be seen from Fig. 15, with the increase of velocity, convection gradually enhances the composition gradient and consequently enhances the molecular diffusion which pulls the composition off the chemistry-based slow manifold. We observe that for  $v = 1$ , where the convection time scale (order of 1) is much larger than the fast chemical time scale (order of 0.01), the compositions still lie close to the chemistry-based slow manifold. For this regime, as may be seen from Fig. 16, after the initial transient, the dominant balance in the normal subspace of the chemistry-based slow manifold is between molecular diffusion and chemical reaction, i.e., the implication Eq. (41) of the close-parallel assumption is still valid even when convection is present. The components of convection and rate of change in the normal subspace are negligible as implied by the close-parallel assumption. Moreover, as may be seen from Fig. 17, the close-parallel assumption (Eq. (44)) provides an accurate reduced description of the full system. However, as shown in Fig. 15, when convec-

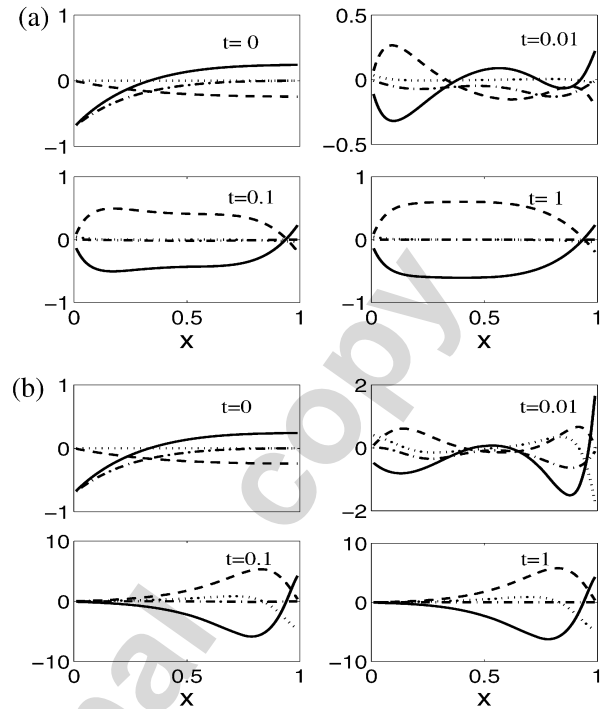


Fig. 16. The balance of rate of change, molecular diffusion, and reaction in the normal subspace of the chemistry-based slow manifold from the system Eq. (51) with different values of velocity: (a)  $v = 1$ ; (b)  $v = 10$ . All the other parameters including boundary and initial conditions are the same as those for Case 4 of the system Eq. (29) in Table 1 with  $\varepsilon = 0.01$  and  $D_1 = 1$ . Solid line: molecular diffusion; dashed line: reaction; dash-dotted line: rate of change; dotted line: convection.

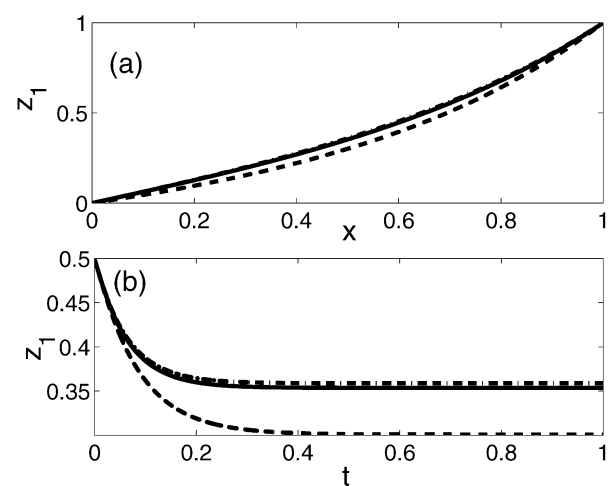


Fig. 17. Results from different descriptions of the system Eq. (51) with velocity  $v = 1$ . All the other parameters including boundary and initial conditions are the same as those for Case 4 of the system Eq. (29) in Table 1 with  $\varepsilon = 0.01$  and  $D_1 = 1$ . (a) Distribution of  $z_1$  at  $t = 1$ ; (b) evolution of  $z_1$  at  $x = 0.5$ . Solid line: full PDE solution; dashed line: reduced description with first approximation; dash-dotted line: reduced description with close-parallel assumption.

tion becomes larger and therefore the convection time scale become smaller (for example,  $v = 10$ ), convection greatly enhances the diffusion process such that the compositions are far away from the slow manifold and consequently the close-parallel assumption and its implication are not valid. As may be seen from Fig. 16, when  $v = 10$ , the balance between diffusion and reaction does not hold in some region.

## 5. Conclusion

In this study, the issues arising from the use of chemistry-based slow manifolds in inhomogeneous reactive flows are addressed. For a class of reaction–diffusion systems, by perturbation analysis, an expression is obtained for the composition perturbation off the chemistry-based slow manifold. It reveals that there are three different mechanisms that pull compositions off the chemistry-based slow manifold in an inhomogeneous reactive flow: noninvariance, dissipation–curvature, and differential diffusion. Correspondingly, these three perturbations introduce three usually nontrivial terms in the evolution equation of the reduced composition variables. Hence the first approximation, which simply neglects these small perturbations (and hence neglects the usually nontrivial terms in the evolution equation of the reduced composition variable), is only accurate under some particular circumstances.

In this study, from different perspectives, we demonstrate the close-parallel phenomena, which provides support for the close-parallel assumption in Ren et al. [24]. We show that due to the noninvariance of the chemistry-based slow manifold, the reaction trajectory in a homogeneous systems is pulled off the slow manifold in the initial transient and then evolves close to and parallel to the slow manifold. We also show that in the regime where fast chemical time scales are much smaller than those of transport processes, the transport processes only slightly perturb the compositions off the chemistry-based slow manifold. After the initial transient, the compositions in an inhomogeneous reactive flow tend to lie on a manifold that is close to and parallel to the chemistry-based slow manifold.

Moreover, we quantitatively validate the close-parallel assumption proposed by Ren et al. [24] to account for the noninvariance, dissipation–curvature, and differential diffusion effects in the reduced description. We illustrate the balance between the molecular diffusion and chemical reactions in the normal subspace of the slow manifold. Based on this balance, composition perturbations are computed and the above three effects can be incorporated in the evolution equation of the reduced composition variables.

It is demonstrated that after the noninvariance effect and transport–chemistry coupling are accounted for, the reduced description agrees well with the full reactive system.

For simplicity of exposition, in this paper, we consider only inhomogeneous flows with constant and uniform enthalpy and pressure. However, the extension to variable pressure and enthalpy is straightforward. For example, for an inhomogeneous reactive flow with nonuniform enthalpy, it is easy to show that the heat transfer and heat loss introduce additional coupling terms into the reduced description of the same form as those in the species equations.

## Acknowledgments

This work has benefited substantially from discussions with Professor Sau-Hai Lam of Princeton University, who also provided valuable comments and suggestions on the paper. The authors appreciate the invaluable comments from the reviewers. Helpful comments were also received from Alexander Vladimirov, John Guckenheimer, Stephen Vavasis, Steve Lantz, and Paul Chew. This research is supported by the National Science Foundation through Grant CTS-0426787.

## References

- [1] U. Maas, S.B. Pope, *Combust. Flame* 88 (1992) 239–264.
- [2] S.B. Pope, U. Maas, *Simplifying Chemical Kinetics: Trajectory-Generated Low-Dimensional Manifolds*, FDA 93-11, Cornell University, 1993.
- [3] M.J. Davis, R.T. Skodje, *J. Chem. Phys.* 111 (1999) 859–874.
- [4] S.J. Fraser, *J. Chem. Phys.* 88 (1988) 4732–4738.
- [5] M.R. Roussel, S.J. Fraser, *J. Chem. Phys.* 93 (1990) 1072–1081.
- [6] M.R. Roussel, S.J. Fraser, *J. Phys. Chem.* 97 (1993) 8316–8327.
- [7] Z. Ren, S.B. Pope, *Proc. Combust. Inst.* 30 (2005) 1293–1300.
- [8] Z. Ren, S.B. Pope, *Combust. Theory Modelling* 10 (2006) 361–388.
- [9] Z. Ren, S.B. Pope, A. Vladimirov, J.M. Guckenheimer, *J. Chem. Phys.* 124 (2006) 114111.
- [10] M. Bodenstein, S.C. Lind, *Z. Phys. Chem. Stoichiomet. Verwandtschaftsl.* 57 (1906) 168–175.
- [11] J.Y. Chen, *Combust. Sci. Technol.* 57 (1988) 89–94.
- [12] M.D. Smooke (Ed.), *Reduced Kinetic Mechanisms and Asymptotic Approximations for Methane–Air Flames*, Lecture Notes in Physics, vol. 384, Springer-Verlag, Berlin, 1991.
- [13] Z. Ren, S.B. Pope, *Combust. Flame* 137 (2004) 251–254.

- [14] J.C. Keck, D. Gillespie, *Combust. Flame* 17 (1971) 237–241.
- [15] J.C. Keck, *Prog. Energy Combust. Sci.* 16 (1990) 125–154.
- [16] C.W. Gear, T.J. Kaper, I.G. Kevrekidis, A. Zagaris, *SIAM J. Appl. Dynam. Syst.* 4 (2005) 711–732.
- [17] C.W. Gear, I.G. Kevrekidis, *J. Sci. Comput.* 25 (2005) 17–28.
- [18] H.G. Kaper, T.J. Kaper, *Physica D* 165 (2002) 66–93.
- [19] A.N. Gorban, I.V. Karlin, *Chem. Eng. Sci.* 58 (2003) 4751–4768.
- [20] A.N. Gorban, I.V. Karlin, A.Y. Zinovyevb, *Phys. Rep.* 396 (2004) 197–403.
- [21] S.H. Lam, D.A. Goussis, *Proc. Combust. Inst.* 22 (1988) 931–941.
- [22] S.H. Lam, *Combust. Sci. Technol.* 89 (1993) 375–404.
- [23] S.H. Lam, D.A. Goussis, *Int. J. Chem. Kinet.* 26 (1994) 461–486.
- [24] Z. Ren, S.B. Pope, A. Vladimirovsky, J.M. Guckenheimer, *Proc. Combust. Inst.* (2007), doi:10.1016/j.proci.2006.07.106.
- [25] S.H. Lam, *The Effect of Fast Chemical Reactions on Mass Diffusion*, Report T1953-MAE, Princeton University, 1992.
- [26] S.H. Lam, *Reduced chemistry–diffusion coupling*, in: 11th International Conference on Numerical Combustion, Granada, Spain, April 23–26, 2006. Also, *Combust. Sci. Technol.*, in press.
- [27] S.H. Lam, personal communication, 2006.
- [28] M. Hadjinicolaou, D.A. Goussis, *SIAM J. Sci. Comput.* 20 (1999) 781–810.
- [29] D.A. Goussis, M. Valorani, F. Creta, H.N. Najm, *Prog. Comput. Fluid Dynam.* 5 (2005) 316–326.
- [30] D.A. Goussis, M. Valorani, *J. Comput. Phys.* 214 (2006) 316–346.
- [31] M. Valorani, D.A. Goussis, F. Creta, H.N. Najm, *J. Comput. Phys.* 209 (2005) 754–786.
- [32] M. Valorani, H.N. Najm, D.A. Goussis, *Combust. Flame* 134 (2003) 35–53.
- [33] A.N. Yannacopoulos, A.S. Tomlin, J. Brindley, J.H. Merkin, M.J. Pilling, *Physica D* 83 (1995) 421–449.
- [34] S. Singh, J.M. Powers, S. Paolucci, *J. Chem. Phys.* 117 (2002) 1482–1496.
- [35] H. Bongers, J.A. van Oijen, L.P.H. de Goey, *Proc. Combust. Inst.* 29 (2002) 1371–1378.
- [36] J.A. van Oijen, L.P.H. de Goey, *Combust. Sci. Technol.* 161 (2000) (2002) 113–137.
- [37] S.S. Girimaji, C. Brau, *Theor. Comput. Fluid Dynam.* 17 (2002) 171–188.
- [38] M.J. Davis, *J. Phys. Chem. A* 110 (2006) 5235–5256.
- [39] M.J. Davis, *J. Phys. Chem. A* 110 (2006) 5257–5272.
- [40] S. Singh, Y. Rastigejev, S. Paolucci, J.M. Powers, *Combust. Theory Modelling* 5 (2001) 163–184.
- [41] U. Maas, S.B. Pope, *Proc. Combust. Inst.* 24 (1992) 103–112.
- [42] U. Maas, S.B. Pope, *Proc. Combust. Inst.* 25 (1994) 1349–1356.
- [43] Z. Ren, S.B. Pope, submitted for publication.
- [44] S.B. Pope, *Flow Turb. Combust.* 72 (2004) 219–243.
- [45] A.N. Yannacopoulos, A.S. Tomlin, J. Brindley, J.H. Merkin, M.J. Pilling, *Chem. Phys. Lett.* 248 (1996) 63–70.
- [46] A.N. Yannacopoulos, A.S. Tomlin, J. Brindley, J.H. Merkin, M.J. Pilling, *Phys. Lett. A* 223 (1996) 82–90.
- [47] Q. Tang, S.B. Pope, *Combust. Theory Modelling* 8 (2004) 255–279.
- [48] A. Adrover, F. Cretab, M. Giona, M. Valorani, V. Vitacolonna, *Physica D* 213 (2006) 121–146.
- [49] A. Zagaris, H.G. Kaper, T.J. Kaper, *Multiscale Model. Simul.* 2 (2004) 613–638.
- [50] S.B. Pope, *Turbulent Flows*, Cambridge Univ. Press, Cambridge, UK, 2000.
- [51] N. Peters, *Turbulent Combustion*, Cambridge Univ. Press, Cambridge, UK, 2000.
- [52] P. Deuffhard, J. Heroth, in: F. Keil, W. Mackens, H. Vob, J. Werther (Eds.), *Scientific Computing in Chemical Engineering*, Springer-Verlag, Berlin, 1996.
- [53] Z. Ren, S.B. Pope, in preparation.